DISTRIBUTION CORRECTED ESTIMATION VIA ADVERSARIAL DENSITY WEIGHTED REGRESSION

Anonymous authors
Paper under double-blind review

ABSTRACT

We propose a novel one-step supervised imitation learning (IL) framework called Adversarial Density Regression (ADR). This IL framework aims to correct the policy learned on unknown-quality to match the expert distribution by utilizing demonstrations, without relying on the Bellman operator. Specifically, ADR addresses several limitations in previous IL algorithms: First, most IL algorithms are based on the Bellman operator, which inevitably suffer from cumulative offsets from sub-optimal rewards during multi-step update processes. Additionally, off-policy training frameworks suffer from Out-of-Distribution (OOD) state-actions. Second, while conservative terms help solve the OOD issue, balancing the conservative term is difficult. To address these limitations, we fully integrate a one-step density-weighted Behavioral Cloning (BC) objective for IL with auxiliary imperfect demonstration. Theoretically, we demonstrate that this adaptation can effectively correct the distribution of policies trained on unknown-quality datasets to align with the expert policy's distribution. Moreover, the difference between the empirical and the optimal value function is proportional to the upper bound of ADR's objective, indicating that minimizing ADR's objective is akin to approaching the optimal value. Experimentally, we validated the performance of ADR by conducting extensive evaluations. Specifically, ADR outperforms all of the selected IL algorithms on tasks from the Gym-Mujoco domain. Meanwhile, it achieves an **89.5%** improvement over IQL when utilizing ground truth rewards on tasks from the Adroit and Kitchen domains.

1 INTRODUCTION

Reinforcement Learning (RL) has revolutionized various fields, including robotics learning (Brohan et al., 2023a;b; Bhargava et al., 2020), language modeling (Ouyang et al., 2022; Touvron et al., 2023), and the natural science (Gómez-Bombarelli et al., 2018). Despite its success, RL requires extensive interactions with the environment to obtain the optimal policy, which poses challenges for sample efficiency. One way to address this limitation is by leveraging static RL datasets in offline settings. However, this approach often faces the issue of overestimation of Out-Of-Distribution (OOD) states-actions (Levine et al., 2020). To mitigate this, prior research has introduced conservative methods, such as incorporating regularization terms (Fujimoto et al., 2019a; Wu et al., 2022) in the policy learning objective, or pessimism terms in value function learning objective (Kumar et al., 2020a), helping alleviate the OOD issues. However, offline RL algorithms generally assume that offline datasets contain reward labels. Moreover, striking the balance with conservative terms in offline RL remains difficult, particularly for tasks with sparse rewards (Cen et al., 2024).

On the other hand, when the dataset does not contain rewards, we can utilize Imitation Learning (IL) algorithms to learn near-expert policy by utilizing a large amount of unknown-quality datasets and a small number of demonstrations (Argall et al., 2009). In particular, one of the most common methods is to train a discriminator through generative Adversarial Learning to represent the reward or value functions (Ho and Ermon, 2016), and followed by updating within RL frameworks. However, it is difficult for the discriminator to converge to its optimal value (Kostrikov et al., 2019). Furthermore, sub-optimal reward or value functions can lead to unstable training. On the other hand, there is another approach termed distribution correct estimation (DICE) (Kim et al., 2022; Ma et al., 2022a; Reddy et al., 2019). It corrects the policy's distribution through importance sampling (IS) to make the learned policy closer to the expert's distribution. However, the cumulative offset caused by

suboptimal rewards or values in the process of using the Bellman operator for multi-step updates has not been fundamentally resolved, and balancing conservatism remains challenging.

To address these limitations, we introduce ADR, a streamlined one-step supervised framework derived from Equation 8. The key objective of ADR is to closely align the policy distribution with that of the demonstrations while diverging from the distributions of datasets with unknown-quality. Theoretically, this method effectively shifts the empirical distribution toward the expert distribution in a direct and corrective manner (Proposition 5.2). Moreover, we demonstrate in Proposition 5.3 that the value bound is proportional to the lower bound of ADR's objective. Thus, minimizing ADR's objective leads to convergence towards the optimal policy. In particular, ADR is a one-step supervised IL framework, where all training samples are in-sample, effectively eliminating the challenges of OOD issues. This approach is particularly promising in offline settings, as most RL studies frame the offline RL problem within a Markov Decision Process (MDP) (Kumar et al., 2019; Kostrikov et al., 2021; Haarnoja et al., 2018a; Fujimoto et al., 2019b; van Hasselt et al., 2015). Under the MDP setting, decision-making depends solely on the current observation and policy, independent of historical information. Thus, if the action support is adequately relocated, the policy's performance can be ensured. To validate ADR's effectiveness, we evaluated it across various tasks from the Adroit and Gym-Mujoco domains under the Learning from Demonstration (LfD) setting, where it demonstrated competitive results. Notably, ADR outperformed Implicit Q Learning (IQL) by 89.5% on tasks from the Adroit and Kitchen domains when utilizing ground truth rewards.

Our main contribution is ADR, a novel single-step supervised IL method. Unlike most modern RL-combined IL algorithms, which rely on the Bellman operator and incorporate reward shaping and Q-estimating processes, ADR operates as a single-step supervised learning paradigm, rendering it immune to the accumulated offsets resulting from suboptimal rewards. Meanwhile, ADR neither requires the addition of conservative terms nor extensive hyperparameter parameter tuning during the training process. Meanwhile, compared to traditional single-step IL paradigms such as Behavioral Cloning (BC), ADR can achieve better performance with a limited number of demos based on adversarial density-weighted regression. Therefore, ADR combines the advantages of single-step updates while demonstrating superior performance compared to previous RL-combined IL approaches on the experimental level. Moreover, we prove that optimizing ADR's objective is akin to approaching the demo policy, and our experimental results validate this claim, demonstrating that ADR outperforms the majority of RL-combined approaches across diverse domains.

2 Related Work

Imitation Learning (IL). IL has a long history of development, with well-known algorithms such as BC. However, BC is brittle when demonstrations are scarcity (Ross et al., 2011a). Currently, the more effective IL paradigms are generally of the RL-combined type. Specifically, these type of IL methods encompass various settings, each tailored to specific objectives. Primarily, IL can be categorized based on the imitating objective into Learning from Demonstration (LfD) (Argall et al., 2009; Judah et al., 2014; Ho and Ermon, 2016; Brown et al., 2020; Ravichandar et al., 2020; Boborzi et al., 2022) and Learning from Observation (LfO) (Ross et al., 2011b; Liu et al., 2018; Torabi et al., 2019; Boborzi et al., 2022). Despite RL-combined RL methods have shown improved performance, most RL-combined IL algorithms are based on reward or Q-value estimation. Therefore, this paradigm may suffer from cumulative offsets originating from suboptimal rewards, which can affect the performance of the policy. To overcome this limitation, we introduce ADR that utilizes a density-weighted BC objective to perform single-step updates, effectively mitigating cumulative offsets while preserving high performance as RL-combined methods. Additionally, IL can also be implemented in a supervised learning manner by training a latent information-conditioned policy (Liu et al., 2023a; Zhang et al., 2024). However, they introduce an extra latent condition.

Behavior Policy Modeling. Previously, estimating the support of the behavior policy has been approached using various methods, including Gaussian (Kumar et al., 2019; Wu et al., 2019) or Gaussian mixture (Kostrikov et al., 2021) sampling approaches, Variance Auto-Encoder (VAE) based techniques (Kingma and Welling, 2022; Debbagh, 2023), or accurate sampling via autoregressive language models (Germain et al., 2015). Specifically, the most relevant research to our study involves utilizing VAE to estimate the density-based definition of action support (behavior density) (Fujimoto et al., 2019b; Wu et al., 2022). On the other hand, behavior policy is utilized to regularize the offline training policy (Fujimoto and Gu, 2021), reducing the extrapolation error of

offline RL algorithms, it has also been utilized in offline-to-online setting (Wu et al., 2022; Fujimoto and Gu, 2021; Nair et al., 2021) to ensure the stable online fine-tuning. Different from the previous study, our focus is on using the estimated target density to optimize policy with the ADR objective.

3 PRELIMINARIES

Reinforcement Learning (RL). We consider RL can be represented by a Markov Decision Process (MDP) tuple *i.e.*, $\mathcal{M} := (\mathcal{S}, \mathcal{A}, p_0, r, d_{\mathcal{M}}, \gamma)$, where $\mathcal{S}$ and $\mathcal{A}$ separately denotes observation and action space, $\mathbf{a} \in \mathcal{A}$ and $\mathbf{s} \in \mathcal{S}$ separately denotes state (observation) and action (decision making). $\mathbf{s}_0$ denotes initial observation, p_0 denotes initial distribution, $r(\mathbf{s}_t, \mathbf{a}_t) : \mathcal{S} \times \mathcal{A} \to \mathbb{R}$ denotes reward function. $d_{\mathcal{M}}(\mathbf{s}_{t+1}|\mathbf{s}_t, \mathbf{a}_t) : \mathcal{S} \times \mathcal{A} \to \Delta(\mathcal{S})$ denotes the transition function, $\gamma \in [0, 1]$ denotes the discounted factor. The goal of RL is to obtain the optimal policy π^* that can maximize the accumulated Return *i.e.*, $\pi^* := \arg\max_\pi \sum_{t=0}^{t=T} \gamma^t \cdot r(\mathbf{s}_t, \mathbf{a}_t)$, where $\tau = \big\{\mathbf{s}_0, \mathbf{a}_0, r(\mathbf{s}_0, \mathbf{a}_0), \cdots, \mathbf{s}_k, \mathbf{a}_k, r(\mathbf{s}_k, \mathbf{a}_k), \cdots, \mathbf{s}_T, \mathbf{a}_T, r(\mathbf{s}_T, \mathbf{a}_T)|\mathbf{s}_0 \sim p_0, \mathbf{a}_t \sim \pi(\cdot|\mathbf{s}_t), \mathbf{s}_{t+1} \sim d_{\mathcal{M}}(\cdot|\mathbf{s}_t, \mathbf{a}_t)\big\}$, and T denotes time horizon.

Imitation Learning (IL). In IL problem setting, $r(\mathbf{s}, \mathbf{a})$ is inaccessible, but we have access to a limited number of demonstrations $\mathcal{D}^* = \{\tau^* = \{\mathbf{s}_0, \mathbf{a}_0, \mathbf{s}_1, \mathbf{a}_1, \cdots, \mathbf{s}_k, \mathbf{a}_k, \cdots \mathbf{s}_T, \mathbf{a}_T|\mathbf{a}_t \sim \pi^*(\cdot|\mathbf{s}), \mathbf{s}_0 \sim p_0, \mathbf{s}_{t+1} \sim d_{\mathcal{M}}(\mathbf{s}_{t+1}|\mathbf{s}_t, \mathbf{a}_t)\}\}$, and large amount of unknown-quality dataset $\hat{\mathcal{D}} = \{\hat{\tau}|\hat{\tau} \sim \hat{\pi}\}$. In particular, one of the classical IL methods is behavior cloning (BC), where the objective is to maximize the likelihood of expert decision-making, as follows:

$$\pi_\theta := \arg\max_{\pi_\theta} \mathbb{E}_{(\mathbf{s},\mathbf{a})\sim\mathcal{D}^*}[\log \pi_\theta(\mathbf{a}|\mathbf{s})], \tag{1}$$

however, BC's performance is brittle when $\mathcal{D}^*$ is scarcity (Ross et al., 2011a). Another approach is to recover a policy $\pi(\cdot|\mathbf{s})$ by matching the distribution of the expert policy. Since π^* cannot be directly accessed, previous studies frame IL as a distribution-matching problem. Specifically, the process begins by estimating a reward or Q-function $c(\mathbf{s}, \mathbf{a})$ as follows:

$$c(\mathbf{s}, \mathbf{a}) := \arg\min_c \mathbb{E}_{(\mathbf{s},\mathbf{a})\sim\hat{\mathcal{D}}}[\log(\sigma(c(\mathbf{s}, \mathbf{a})))] + \mathbb{E}_{(\mathbf{s},\mathbf{a})\sim\mathcal{D}^*}[\log(1 - \sigma(c(\mathbf{s}, \mathbf{a})))], \tag{2}$$

where σ denotes the *Sigmoid* function. The empirical policy π_θ is then optimized within a RL framework. However, most of these approaches rely on Adversarial learning (Kostrikov et al., 2019), which often suffers from unstable training caused by sub-optimal reward or value functions.

Definition 1. *(Stationary Distribution) We separately define the γ discounted stationary distribution (state-action occupancy) of expert and non-expert behavior as $d^{\pi^*}(\mathbf{s}, \mathbf{a})$ and $d^\pi(\mathbf{s}, \mathbf{a})$. In particular, $d^\pi(\mathbf{s}, \mathbf{a})$ can be formulated as:*

$$d^\pi(\mathbf{s}, \mathbf{a}) := (1 - \gamma) \sum_{t=0}^{\infty} \gamma^t \cdot \Pr(\mathbf{s} = \mathbf{s}_t, \mathbf{a} = \mathbf{a}_t|\mathbf{s}_0 \sim \mu_0, \mathbf{a}_t \sim \pi(\cdot|\mathbf{s}_t), \mathbf{s}_{t+1} \sim d_{\mathcal{M}}(\cdot|\mathbf{s}_t, \mathbf{a}_t)), \tag{3}$$

Distribution Corrected Estimation (DICE). On the other hand, Distributed Corrected Estimation (DICE) related methods solve the offline setting by utilizing the marginal state distribution divergence reweighed reward, *i.e.*,

$$J_{d^\pi \geq 0} = \mathbb{E}_{d^\pi}[r(\mathbf{s}, \mathbf{a})] - D_{KL}[d^{\pi^*}||d^\pi], \tag{4}$$

correcting the distribution towards the expert distribution, where d^π is marginal distribution that defined in Definition 1. Different from these aforementioned methods, our approach is purely a supervised IL framework that entirely utilizes a density-weighted BC objective to leverage demonstrations to correct the policy distribution learned on unknown-quality datasets toward expert distribution. Nevertheless, our method necessitates the estimation of behavior density as a prerequisite.

Behavior density estimation via Variance Auto-Encoder (VAE). Typically, action support constrain *i.e.*, $D_{\mathrm{KL}}[\pi_\theta||\pi_\beta] \leq \epsilon$ has been utilized to confine the training policy to the support set of the behavior policy π_β (Kumar et al., 2019; Fujimoto et al., 2019b), aiming to mitigate extrapolation error. In this research, we propose leveraging existing datasets and demonstrations to separately learn the target and sub-optimal behavior densities, which are then utilized for ADR. In particular, we

follow Wu et al. to estimate the density of action support with Linear Variance Auto-Encoder (VAE) (as demonstrated VAE-1 in (Damm et al., 2023)) by Empirical Variational Lower Bound (ELBO) :

$$\begin{aligned}\log p_\Theta(\mathbf{a}|\mathbf{s}) &\geq \mathbb{E}_{q_\Phi(\mathbf{z}|\mathbf{a},\mathbf{s})}[\log p_\Theta(\mathbf{a},\mathbf{z}|\mathbf{s})] - D_{\mathrm{KL}}[q_\Phi(\mathbf{a}|\mathbf{s},\mathbf{a})||p(\mathbf{s}|\mathbf{z})] \\ &\stackrel{\text{def}}{=} -\mathcal{L}_{\mathrm{ELBO}}(\mathbf{s},\mathbf{a};\Theta,\Phi),\end{aligned} \tag{5}$$

and computing the policy likelihood through importance sampling during evaluation:

$$\log p_\Theta(\mathbf{a}|\mathbf{s}) \approx \mathbb{E}_{\mathbf{z}^l\sim q_\Phi(\mathbf{z}|\mathbf{s},\mathbf{a})}\left[\frac{1}{L}\sum_{L}\frac{p_\Theta(\mathbf{a},\mathbf{z}^l|\mathbf{s})}{q_\Phi(\mathbf{z}^l|\mathbf{a},\mathbf{s})}\right] \stackrel{\text{def}}{=} \mathcal{L}_{\pi_\beta}(\mathbf{s},\mathbf{a};\Theta,\Phi,L), \tag{6}$$

where $\mathbf{z}^l \sim q_\Phi(\mathbf{z}|\mathbf{s},\mathbf{a})$ is the l_{th} sampled VAE embedding, Θ and Φ are separately encoder's and decoder's parameter, l and L respectively denote the l_{th} sampling index and the total sampling times.

4 Problem Formulation

Notations. Prior to formulating our objective, we first define $P^*(\mathbf{a}|\mathbf{s})$ as the expert behavior density (*The conception of behavior density is proposed by Wu et al. (2022), representing the density probability of the given action* $\mathbf{a}$ *within the expert action support*), and define the sub-optimal behavior density as $\hat{P}(\mathbf{a}|\mathbf{s})$. Meanwhile, we define the training policy as $\pi_\theta(\cdot|\mathbf{s}) : \mathcal{S} \to \mathcal{A}$. Additionally, we denote the stationary distributions of the empirical policy, datasets and expert policy by d^π, $d^\mathcal{D}$ and d^{π^*}, respectively. The Kullback-Leibler (KL) divergence is represented as D_{KL}. where $d^{\pi^*}(\mathbf{s},\mathbf{a})$ can be formulated by replacing π with π^*.

Previous IL algorithms have several limitations: 1) Accumulated offsets can result from using sub-optimal reward or value functions during multi-step updates. Additionally, off-policy frameworks may introduce OOD state-actions. 2) Some off-policy offline frameworks necessitate tuning of hyperparameters to strike a balance between conservatism, and overly conservatism constrains the exploratory capacity of policies, limiting their ability to adapt and improve beyond the demonstrations provided. To overcome these issues, we completely adapt a supervised learning objective ADR to correct the policy distribution on unknown-quality datasets using a small number of demonstrations.

Remark 4.1. *$d^\pi(\mathbf{s}) > 0$ whenever $d^\mathcal{D}(\mathbf{s}) > 0$ is a guarantee that the on-policy samples $\mathcal{D}$ has coverage over the expert state-marginal, and is necessary for IL to succeed. (This remark has been extensively deliberated by Ma et al.)*

Policy Distillation via KL Divergence. Rusu et al. (2016) demonstrates the effectiveness of policy distillation by minimizing the KL divergence between the training policy π_θ and the likelihood of teacher policy set $\pi_i \in \Pi$, *i.e.*, $\pi := \arg\min_{\pi_\theta} D_{\mathrm{KL}}[\pi_\theta||\pi_i]\big|_{\pi_i\in\Pi}$. Meanwhile, if the condition mentioned in Remark 4.1 is held, we can directly achieve expert behavior through distillation, *i.e.*,

$$\pi := \arg\min_{\pi_\theta} D_{\mathrm{KL}}[\pi_\theta||P^*]. \tag{7}$$

however, it's insufficient to mimic the expert behavior by minimizing the KL divergence between $\pi_\theta(\mathbf{a}|\mathbf{s})$ and $P^*(\mathbf{a}|\mathbf{s})$, since the limited demonstrations aren't sufficient to help to estimate a good $P^*(\cdot|\mathbf{s})$. To address this limitation, we propose Adversarial Density Regression (ADR), a supervised learning algorithm that utilizes a limited number of demonstrations to correct the distribution learned by the policy on datasets of unknown-quality, thereby bringing it closer to the expert distribution.

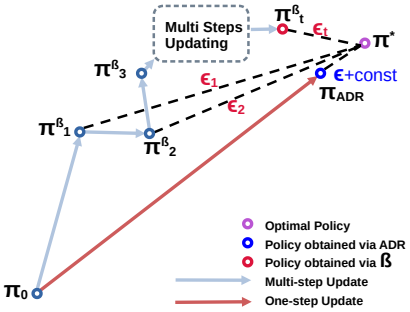

Figure 1: Blue path based on Bellman operator $\mathcal{B}$, the distance from the optimal policy varies with all iterations. Red path, the precise path to the optimal policy.

Adversarial Density Regression (ADR). In particular, beyond aligning π_θ with the expert distribution P^*, we also push π_θ away from the empirical distribution $\hat{P}$, as formulated in Equation 8. This approach is formalized as Adversarial Density Regression (ADR) in Definition 2. The primary advantage of ADR lies in its independence from the Bellman operator, and it's an one-step supervised learning paradigm. Therefore, ADR won't be impacted by the cumulative offsets that introduced during multi-step updates (demonstrated in Figure 1), ensuring a more stable and reliable learning process.

Definition 2 (Adversarial Density Regression (ADR)). *Given expert behavior density $P^*(\mathbf{a}|\mathbf{s})$ and sub-optimal behavior density $\hat{P}(\mathbf{a}|\mathbf{s})$, we formulate the process of Adversarial Policy Divergence, where π_θ approaches the expert behavior while diverging from the sub-optimal behavior, as follows:*

$$\pi_\theta := \arg\min_{\pi_\theta} \mathbb{E}_{\mathcal{D}}[D_{\mathrm{KL}}[\pi_\theta||P^*] - D_{\mathrm{KL}}[\pi_\theta||\hat{P}]], \tag{8}$$

Density Weighted Regression (DWR). However, it's computing in-efficient to directly compute the objective formulated in Definition 2. But, according to Theorem 4.2, we can instead computing:

$$\pi_\theta := \arg\min_{\pi_\theta} \mathbb{E}_{(\mathbf{s},\mathbf{a})\sim\mathcal{D}}\big[\mathcal{W}(\hat{P}, P^*) \cdot ||\pi_\theta(\cdot|\mathbf{s}) - \mathbf{a}||^2\big] \tag{9}$$

to replace Equation 8, where $\mathcal{W}(\hat{P}, P^*) = \log \frac{\hat{P}(\mathbf{a}|\mathbf{s})}{P^*(\mathbf{a}|\mathbf{s})}\big|_{(\mathbf{s},\mathbf{a})\sim\mathcal{D}}$ termed **density weight**.

Theorem 4.2 (Density Weight). *Given expert log behavior density $\log P^*(\mathbf{a}|\mathbf{s}) : \mathcal{S} \times \mathcal{A} \to \mathbb{R}$, sub-optimal log behavior density $\log \hat{P}(\mathbf{a}|\mathbf{s}) : \mathcal{S} \times \mathcal{A} \to \mathbb{R}$, and the empirical policy $\pi_\theta : \mathcal{S} \to \mathcal{A}$, offline dataset $\mathcal{D}$. Minimizing the KL divergence between $\pi_\theta(\mathbf{a}|\mathbf{s})$ and $P^*(\mathbf{a}|\mathbf{s})$, while maximizing the KL divergence between $\pi_\theta(\mathbf{a}|\mathbf{s})$ and $\hat{P}(\mathbf{a}|\mathbf{s})$, i.e.Equation 8. is equivalent to:*

$$\pi_\theta := \arg\min_{\pi_\theta} \mathbb{E}_{(\mathbf{s},\mathbf{a})\sim\mathcal{D}}\big[\log \frac{P^*(\mathbf{a}|\mathbf{s})}{\hat{P}(\mathbf{a}|\mathbf{s})} \cdot ||\pi_\theta(\cdot|\mathbf{s}) - \mathbf{a}||^2\big], \tag{10}$$

Proof of Theorem 4.2, see Appendix D.1.

Meanwhile, to further address the limitations of BC's tendency to overestimate given state-action pairs, we propose minimizing the upper bound of Equation 9 during each update epoch. This approach serves as an alternate real optimization objective, mitigating the overestimation issues *i.e.*,

$$\min_{\pi_\theta} J(\pi_\theta) = \min_{\pi_\theta} \mathbb{E}_{\beta_{\mathcal{D}}\sim\mathcal{D}}\mathbb{E}_{(\mathbf{s},\mathbf{a})\sim\beta_{\mathcal{D}}}\big[\mathcal{W}(\hat{P}, P^*) \cdot ||\pi_\theta(\cdot|\mathbf{s}) - \mathbf{a}||^2\big] \tag{11}$$

$$(\textbf{Cauchy's Inequality}) \leq \min_{\pi_\theta} \mathbb{E}_{\beta_{\mathcal{D}}\sim\mathcal{D}}\mathbb{E}_{(\mathbf{s},\mathbf{a})\sim\beta_{\mathcal{D}}}\big[\mathcal{W}(\hat{P}, P^*)\big] \cdot \mathbb{E}_{(\mathbf{s},\mathbf{a})\sim\beta_{\mathcal{D}}}\big[||\pi_\theta(\cdot|\mathbf{s}) - \mathbf{a}||^2\big], \tag{12}$$

where $\beta_{\mathcal{D}} \in \mathcal{D}$ denotes a batch sampled offline dataset during the offline training process.

5 Theoretical Analysis of Adversarial Density Regression

In this section, we further conduct a theoretical analysis to demonstrate the convergence of ADR.

Assumption 5.1. *Suppose the policy extracted from Equation 12 is π, we separately define the state marginal of the dataset, empirical policy, and expert policy as $d^{\mathcal{D}}$, d^{π} and d^{π^*}, they satisfy this relationship:*

$$D_{KL}[d^{\pi}||d^{\pi^*}] \leq D_{KL}[d^{\mathcal{D}}||d^{\pi^*}] \tag{13}$$

Proposition 5.2 (Policy Convergence of ADR). *Assuming Equation 8 can finally converge to ϵ via minimizing Equation 10, meanwhile, assuming Assumption D.2 is held. Then $\mathbb{E}_{(\mathbf{s},\mathbf{a})\sim\hat{\mathcal{D}}}[D_{KL}(\pi||\pi^*)] \to \frac{M}{2n} \cdot \sqrt{\log\frac{2}{\delta}} + \Delta C + \epsilon$.*

Proposition 5.3. *(Value Bound of ADR) Given the empirical policy π and the optimal policy π^*, let $V^{\pi}(\rho_0)$ and $V^{\pi^*}(\rho_0)$ separately denote the value network of π and π^*, and given the discount factor γ. Meanwhile, let R_{max} as the upper bound of the reward function i.e., $R_{max} = \max ||r(\mathbf{s},\mathbf{a})||$. Based on the Assumption D.7, Assumption D.2, Lemma D.8, and Proposition 5.2, we can obtain:*

$$|V^{\pi}(\rho_0) - V^{\pi^*}(\rho_0)| \leq \underbrace{\frac{R_{max}}{1-\gamma} D_{TV}[d^*(\mathbf{s})||d^{\mathcal{D}}(\mathbf{s})]}_{\textbf{w.l.o.g}} + \frac{2 \cdot R_{max}}{1-\gamma} \cdot \sqrt{2 \cdot (\frac{M}{2n} \cdot \sqrt{\log\frac{2}{\delta}} + \Delta C + \epsilon)}, \tag{14}$$

where, $\Delta C = C_1 - C_2$ is a constant term, dependent on the state distribution. δ originates from Assumption D.2, $n = |\mathcal{D}^*|$, $M := \arg\max_{X_i}\{X_i = \pi^*(\mathbf{a}_t|\mathbf{s}_t) \log \frac{\pi^*(\mathbf{a}_t|\mathbf{s}_t)}{\hat{\pi}(\mathbf{a}_t|\mathbf{s}_t)} | (\mathbf{s}_t, \mathbf{a}_t) \sim \mathcal{D}^*\}$.

Proof of Proposition 5.2 and Proposition 5.3, see Appendix D.4 and Appendix D.9.

From Proposition 5.2, we can infer that if Equation 8 converges to a small threshold ϵ, the KL divergence between the likelihood of π and π^* on unknown-quality data will converge to the same order of magnitude *i.e.*, $O(\epsilon)$. This implies that the action distribution learned by the π will become closer to the π^*, as long as the states in the unknown-quality data sufficiently cover the states of the π^*, π will learn as many expert decisions as possible. At the same time, in Proposition 5.3, we further prove that the regret of policy π is proportional to the convergence upper bound of Equation 8. Therefore, minimizing Equation 8 implies that $V^{\pi}(\rho_0)$ will converge to the $V^{\pi^*}(\rho_0)$ considering the current dataset. Specifically, the first term on the left-hand side of Equation 14 is determined by the quality of the dataset, which is generally applicable to all algorithms (**w.l.o.g**). However, the second term is unique to ADR, as the supervised optimization objective of ADR aligns with maximizing $V^{\pi}(\rho_0)$. Therefore, minimizing ADR's objective can bring π closer to π^*

Policy Distribution Analysis. To validate the near-optimal policy convergence, we visualize the policy distribution of both the behavior learned by ADR and expert behavior (sampled from dataset) in Figure 2. Remarkably, utilizing solely the `medium-replay` dataset, ADR is able to comprehensively cover the expert behavior, demonstrating its efficacy in mimicking the expert policy, thus validaing our claim in Proposition 5.2.

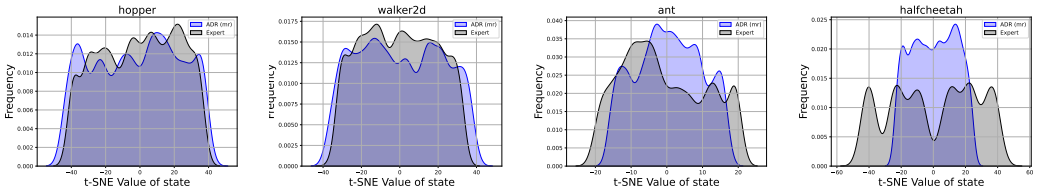

Figure 2: Policy Distribution. We sequentially sampled 500 samples $\tau_{\texttt{sampled}} = \{(\mathbf{s}_t, \mathbf{a}_t)|(\mathbf{s}_t, \mathbf{a}_t) \sim \mathcal{D}_{\texttt{exp}}\}_{t=0}^{t=500}$ from the expert dataset $\mathcal{D}_{\texttt{exp}}$. At the same time, we generated 500 actions based on the policy learned from ADR *i.e.*, $\tau_{\texttt{generate}} = \{\mathbf{a}_t := \pi_\theta(\cdot|\mathbf{s}_t)|\mathbf{s}_t \in \tau_{\texttt{sampled}}\}$. Then, we reduced the dimensions of actions from all $\tau_{\texttt{sampled}}$ and $\tau_{\texttt{generate}}$ using t-SNE and plot the KDE curve.

6 METHODS

To alleviate the constraint posed by the scarcity of demonstrations, we introduce Adversarial Density Estimation (ADE).

Adversarial Density Estimation (ADE). Specifically, during the training stage, we utilize the ELBO of VAE to estimate the density probability of state-action pair in action support *i.e.*, Equation 6. Additionally, to alleviate the limitation of demonstrations' scarcity, we utilize adversarial learning (AL) in density estimation. This involves maximizing the density probability of expert offline samples while minimizing the density probability of sub-optimal offline samples to improve the estimation of expert behavior density. (Θ^* *doesn't mean the optimal parameter, instead, it means the parameters of VAE model utilized to estimate on expert samples*) :

$$\mathcal{J}_{\texttt{ADE}}(\Theta^*) = \mathbb{E}_{(\mathbf{s},\mathbf{a})\sim\pi^*}\left[\sigma(P_{\Theta^*}(\mathbf{a}|\mathbf{s}))\right] - \mathbb{E}_{(\mathbf{s},\mathbf{a})\sim\hat{\pi}}\left[\sigma(P_{\Theta^*}(\mathbf{a}|\mathbf{s}))\right], \tag{15}$$

Therefore, the expert density's objective can be formulated as :

$$\mathcal{J}(\Theta^*) = \mathbb{E}_{(\mathbf{s},\mathbf{a})\sim\pi^*}\left[\mathcal{L}_{\text{ELBO}}(\mathbf{s},\mathbf{a};\Theta^*,\Phi^*)\right] + \lambda \cdot \mathcal{J}_{\texttt{ADE}}(\Theta^*). \tag{16}$$

Accordingly, the objective for non-expert density can be formulated by substituting Θ^* and Φ^* in Equation 16 with $\hat{\Theta}$ and $\hat{\Phi}$. However, in practical implementations, we find that setting $\lambda = 0$ is sufficient to achieve good performance for sub-optimal behavior density.

Density Weighted Regression (DWR). After using ADE and obtaining the converged VAE estimators $P_{\Theta^*}(\mathbf{a}|\mathbf{s})$ and $P_{\hat{\Theta}}(\mathbf{a}|\mathbf{s})$. We freeze the parameter of these estimators, then approximate the

density weight $W(\hat{P}, P^*) = \log \frac{\hat{P}(\mathbf{a}|\mathbf{s})}{P^*(\mathbf{a}|\mathbf{s})}$ using importance sampling:

$$\begin{aligned} \log \frac{\hat{P}(\mathbf{a}|\mathbf{s})}{P^*(\mathbf{a}|\mathbf{s})}\Big|_{(\mathbf{s},\mathbf{a})\sim\mathcal{D}} &\approx \log p_{\hat{\Theta}}(\mathbf{a}|\mathbf{s}) - \log p_{\Theta^*}(\mathbf{a}|\mathbf{s})\Big|_{(\mathbf{s},\mathbf{a})\sim\mathcal{D}} \\ &\approx \mathcal{L}_{\pi_\beta}(\mathbf{s},\mathbf{a};\hat{\Theta},\hat{\Phi},L) - \mathcal{L}_{\pi_\beta}(\mathbf{s},\mathbf{a};\Theta^*,\Phi^*,L)\big|_{(\mathbf{s},\mathbf{a})\sim\mathcal{D}}, \end{aligned} \tag{17}$$

and then bring density weight into Equation 11 or 12, optimizing policy via gradient decent *i.e.*, $\theta \leftarrow \theta - \eta \cdot \nabla_\theta \mathcal{J}(\pi_\theta)$, where η denotes learning rate (lr).

6.1 Practical Implementation

ADR comprises VAE Pre-training (Algorithm 1) and policy training (Algorithm 2) stages. During the VAE pre-training stage, we utilize VQ-VAE to separately estimate the target density $P^*(\mathbf{a}|\mathbf{s})$ and the suboptimal density $\hat{P}(\mathbf{a}|\mathbf{s})$ by minimizing Equation 12 (or Equation 16) and the VQ loss (van den Oord et al., 2018). During the policy training stage, we optimize the Multiple Layer Perception (MLP) policy π_θ by using Equation 9. For more details about our model architecture and more hyper-parameter settings, please refer to Appendix. In terms of evaluation. We compute the normalized D4rl (normalized) score with the same method as Fu et al., and our experimental result is obtained by averaging the highest score in multiple runs.

Algorithm 1 VAE Pretraining

Require: VAE (density estimator) parameterized by (Θ^*, Φ^*) for expert dataset, VAE parameterized by $(\hat{\Theta}, \hat{\Phi})$ for unknown-quality dataset. Empirical policy $\pi_\theta(\cdot|\mathbf{s})$, unknown-quality offline datasets $\hat{\mathcal{D}}$, demonstrations $\mathcal{D}^*$; VAE training epochs $N_{\textit{VAE train}}$ and policy training epochs $N_{\textit{policy train}}$.

1: **while** $t_1 \leq N_{\textit{VAE train}}$ **do**
2: Sample batch sub-optimal trajectory $\hat{\tau}$ from $\hat{\mathcal{D}}$, and sampling batch expert trajectory τ^* from $\mathcal{D}^*$.
3: update (Θ^*, Φ^*) by Equation 16. Replace (Θ^*, Φ^*) in Equation 16 with $(\hat{\Theta}, \hat{\Phi})$, and update $(\hat{\Theta}, \hat{\Phi})$.
4: **end while**

Algorithm 2 Training Policy

Require: pre-trained density estimators $\hat{P}$, P^*, and datasets $\mathcal{D} = \hat{\mathcal{D}} \cup \mathcal{D}^*$

1: **while** $t_2 \leq N_{\textit{policy train}}$ **do**
2: Computing $\mathcal{W}(\hat{P}, P^*) = \log \frac{P_{\hat{\Phi}}(\mathbf{a}|\mathbf{s})}{P_{\Phi^*}(\mathbf{a}|\mathbf{s})}$.
3: Bring $\mathcal{W}(\hat{P}, P^*)$ to Equation 12 or 9 and updating π_θ.
4: **end while**

7 Evaluation

Our experiments are designed to answer: 1) Does ADR outperform prvious IL approaches (include DICE)? 2) Is it necessary to use an adversarial approach to assist in estimating the target behavior density? 3) Is it necessary to use the density-weighted form to optimize the policy?

Datasets. The majority of our experimental setups are centered around Learning from Demonstration (LfD). For convenience, we denote using n demonstrations to conduct experiments under the LfD setting as LfD (n). We test our method on various domains, including Gym-Mujoco, Androit, and Kitchen domains (Fu et al., 2021). Specifically, the datasets from the Gym-Mujoco domain include `medium` (`m`), `medium-replay` (`mr`), and `medium-expert` (`me`) collected from environments including `Ant`, `Hopper(hop)`, `Walker2d(wal)`, and `HalfCheetah(che)`, and the demonstrations are 5 expert trails from the respective environments. For the `kitchen` and `androits` domains, we rank and sort all trials by their return, and sample the trial with the highest return as demonstration. *The content inside the parentheses* `()` *represents an abbreviation.*

Baselines. The majority selected baselines are shown in Table 3. Specifically, when assessing the Gym-Mujoco domain, the baselines encompass ORIL, SQIL, IQ-Learn, ValueDICE, DemoDICE, SMODICE utilized RL-based weighted BC approaches to update. Additionally, we also compared with previous competitive contextualized BC framework CEIL. When test on kitchen or androits domains, we compared our methods with IL algorithms including OTR and CLUE that utilize reward relabeling approach, and policy optimization via Implicit Q Learning (IQL) (Kostrikov et al., 2021), besides, we also compare ADR with Conservative Q Learning (CQL) (Kumar et al., 2020b) and IQL utilizing ground truth reward separately denoted CQL (oracle) and IQL (oracle), where oracle

Table 1: **Previous IL approaches**. We summarize the majority of previous IL approaches here. Specifically, most of these methods involve estimating the reward or value function and are followed by optimizing with the weighted BC objective.

Algorithm	Optimizing framework	estimating Target	Methods for Target estimating	Weighted BC
OTR (Luo et al., 2023)	IQL (Kostrikov et al., 2021)	$r(\mathbf{s}, \mathbf{a})$	Wasserstein Distance	✔
SQIL (Reddy et al., 2019)	IQL	$r(\mathbf{s}, \mathbf{a})$	Const Reward	✔
CLUE (Liu et al., 2023b)	IQL	$r(\mathbf{s}, \mathbf{a})$	L_2 distance	✔
IQ-Learn (Garg et al., 2022)	Inverse SAC (Haarnoja et al., 2018b)	$r(\mathbf{s}, \mathbf{a})$	Distribution Matching	✗
OIRL (Zolna et al., 2020)	Q-weighted BC	$r(\mathbf{s}, \mathbf{a})$	Distribution Matching	✔
ValueDice (Kostrikov et al., 2019)	Weighted BC	-	DICE	✔
Demodice (Kim et al., 2022)	Weighted BC	-	DICE	✔
SMODICE (Ma et al., 2022a)	Weighted BC	-	DICE	✔
ABC (Sasaki and Yamashina, 2021)	Adversarial Learning	-	-	✗
Noisy BC (Sasaki and Yamashina, 2021)	Behavior Cloning	-	-	✗
CEIL (Liu et al., 2023a)	Hindsight Information Correction	$\mathbf{z}^*$	Latent Expert Distribution Correction	✗
ADR (ours)	Density Weighted BC	$\hat{P}(\mathbf{a}\|\mathbf{s})$ and $P^*(\mathbf{a}\|\mathbf{s})$	ADE+ELBO of VAE	✔

denotes ground truth reward. We do not compare ADR with ABC and Noisy BC because our ablations (`Max ADE`, Noisy Test) have included settings with similar objectives.

7.1 Majority experimental results

Table 2: **Experimental results of Kitchen and Androits domains.** We test ADR on androits and kitchen domains and average the normalized D4rl score across multiple seeds. In particular, the experimental results of BC, CQL (oracle), and IQL (oracle) are directly quoted from Kostrikov et al. (2021), and results of IQL (OTR) on adroit domain are directly quoted from Luo et al., where oracle denotes ground truth reward.

IL Tasks (`LfD (1)`)	**BC**	**CQL (oracle)**	**IQL (oracle)**	**IQL (OTR)**	**IQL (CLUE)**	**ADR**
`door-cloned`	0.0	0.4	1.6	0.01	0.02	**4.8±1.1**
`door-human`	2	9.9	4.3	5.92	7.7	**12.6±3.9**
`hammer-cloned`	0.6	2.1	2.1	0.88	1.4	**17.6±3.3**
`hammer-human`	1.2	4.4	1.4	1.79	1.9	**21.7±11.8**
`pen-cloned`	37	39.2	37.3	46.87	59.4	**84.4±19.2**
`pen-human`	63.9	37.5	71.5	66.82	82.9	**120.6±10.3**
`relocate-cloned`	-0.3	-0.1	-0.2	-0.24	-0.23	**-0.2±0.0**
`relocate-human`	0.1	0.2	0.1	0.11	0.2	**2.0±1.4**
Total (Androit)	104.5	93.6	118.1	122.2	153.3	**263.5**
`kitchen-mixed`	51.5	51.0	51.0	50.0	-	**87.5±1.8**
`kitchen-partial`	38.0	49.8	46.3	50.0	-	**80.6±2.7**
`kitchen-completed`	65.0	43.8	62.5	50.0	-	**95.0±0.0**
Total (Kitchen)	104.5	144.6	159.8	150.0	-	**263.1**
Total (Kitchen&Android)	259	238.2	277.9	272.2	-	**526.6**

LfD on Androits and kitchen domains. We test ADR on tasks sourced from Adroit and Kitchen domains. In particular, during the training process, we utilize single trajectory with the highest Return as a demonstration. The experimental results are summarized in Table 2, ADR achieves an impressive summed score of **526.6** points, representing an improvement of **89.5%** compared to IQL (oracle), **121.1%** compared to CQL (oracle), and surpassing all IL baselines, thus showcasing its competitive performance in long-horizon IL tasks. Meanwhile, these competitive experimental results also validate our claim that ADR, which optimizes policy in a single-step manner, can avoid the cumulative bias associated with multi-step updates using biased reward/Q functions within the RL framework. Moreover, this experiment also indicates its feasibility to utilize ADR to conduct LfD without introducing extra datasets as demonstrations.

LfD on Gym-Mujoco domain. The majority of the experimental results on the tasks sourced from the Gym-Mujoco domain are displayed in Table 3. We utilized 5 expert trajectories as demonstrations and conducted ILD on all selected tasks. ADR achieves a total of **1008.7** points, surpassing most reward estimating and Q function estimating approaches. Therefore, the performance of our

Table 3: **Experimental results of Gym-Mujoco domain.** We utilize 5 expert trajectories as a demonstration to conduct LfD setting IL experiment, our experimental results are averaged multiple times of runs. In particular, `m` denotes `medium`, `mr` denotes `medium-replay`, `me` denotes `medium-expert`.

LfD (5)	**ORIL (TD3+BC)**	**SQIL (TD3+BC)**	**IQ-Learn**	**ValueDICE**	**DemoDICE**	**SMODICE**	**CEIL**	**ADR**
`hopper-me`	51.2	5.9	21.7	72.6	63.7	64.7	80.8	**109.1±3.2**
`halfcheetah-me`	79.6	11.8	6.2	1.2	59.5	63.8	33.9	**74.3±2.1**
`walker2d-me`	38.3	13.6	5.2	7.4	101.6	55.4	99.4	**110.1±0.2**
`Ant-me`	6.0	-5.7	18.7	30.2	112.4	112.4	85.0	**132.7±0.3**
`hopper-m`	42.1	45.2	17.2	59.8	50.2	54.1	94.5	69.0±1.1
`halfcheetah-m`	45.1	14.5	6.4	2	41.9	42.6	45.1	44.0±0.1
`walker2d-m`	44.1	12.2	13.1	2.8	66.3	62.2	103.1	86.3±1.7
`Ant-m`	25.6	20.6	22.8	27.3	82.8	86.0	99.8	**106.6±0.5**
`hopper-mr`	26.7	27.4	15.4	80.1	26.5	34.9	45.1	**74.7±1.7**
`halfcheetah-mr`	2.7	15.7	4.8	0.9	38.7	38.4	43.3	39.2±0.1
`walker2d-mr`	22.9	7.2	10.6	0	38.8	40.6	81.1	67.3±4.7
`Ant-mr`	24.5	23.6	27.2	32.7	68.8	69.7	101.4	95.4±1.1
Total (Gym-Mujoco)	408.8	192	169.2	316.9	751.2	724.7	912.5	**1008.7**

approach on continuous control has been validated. In particular, 1) ADR performs better than ORIL, IQL-Learn demonstrating the advantage of ADR over reward estimating+RL approaches. 2) The superior performance of ADR compared to SQIL, DemoDice, SMODICE, ValueDice highlights the density weights over other regressive forms.

7.2 Ablations

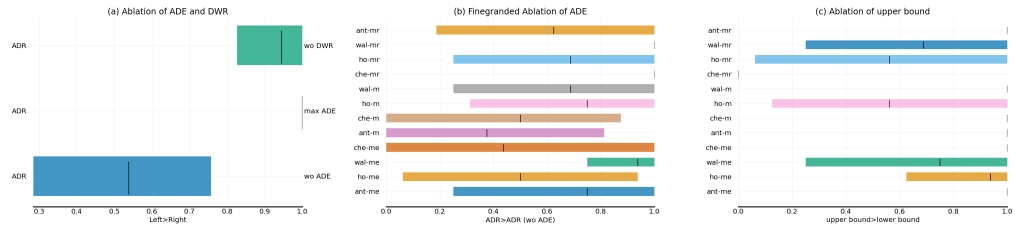

Figure 3: Ablation Results. We utilized the reliable library proposed by Agarwal et al. to conduct our experiments. The results show that the experimental setting on the left side performed better with a higher probability. Specifically, in (a) we removed part of modules *i.e.*, ADE or DWR from ADR and observed a reduction in performance. In (b), we further conducted comparisons among all tasks. Regarding (c), we carried out a fine-grained comparison of the upper and lower bounds of Equation 10 among all tasks. Note, (a) The left and right y-axes represent the selected algorithms A and B, respectively, while the x-axis represents the confidence in A>B. (b, c) involve comparisons between two algorithms, and left y-axis indicates selected tasks.

Ablation of ADE and DWR. To demonstrate the effectiveness of ADE, we excluded ADE *i.e.*, $J_{\texttt{ADE}}(\Theta^*)$ from ADR during the VAE training process. Subsequently, we optimized by maximizing the target behavior density and minimizing the sub-optimal behavior density, and we name this experimental setting as ADR (wo ADE), as shown in Figure 3 (a). ADR (wo ADE) performs better than ADR with over 50% confidence, validating the improvement brought by ADE. Meanwhile, in order to demonstrate the necessity of DWR, we 1) conducted an ablation by removing DWR, denoted as ADR (wo DWR), and found that ADR performs better than ADR (wo DWR) over 95% confidence. This indicates that DWR is necessary for ADR. 2) Optimizing the policy by solely maximizing the expression $\mathcal{L}_{\pi_\beta}(\mathbf{s}, \pi_\theta(\cdot|\mathbf{s}); \Theta^*, \Phi^*, L)|_{\mathbf{s}\sim\mathcal{D}}$, which is termed as `max ADE`, as shown in Figure 3 (a). According to the results, ADR performs better than `max ADE` with over 90% confidence. Therefore, we can't optimize the policy solely by utilizing ADE and maximizing likelihood. Besides, we observe that it won't bring an overwhelming decrease by removing ADE, therefore, we further conduct fine-grand comparison across all tasks from Gym-mujoco domain, and we observe that ADR performs better than ADR (wo ADE) across all selected `mr` tasks, but lower than 50% confidence across several `m` or `me` tasks. Therefore, ADE is essential for training with lower-quality $\hat{\mathcal{D}}$, and won't bring too much improvement for training with higher-quality $\hat{\mathcal{D}}$.

Ablation of the upper bound of ADR. To clearly demonstrate the necessity of Equation 12, we conducted a detailed comparison across all selected Gym-mujoco tasks. As shown in Figure 3 (c), optimizing the upper bound achieved better performance across 11 out

of 12 tasks (except for `che-mr`) from the Gym-mujoco domain with over 50% confidence. Therefore, it is much more effective to optimize Equation 12 rather than Equation D.1.

Robustness to demonstrations' noisy. In order to validate that ADR is robustness to the demonstrations' noise, we choose `hop-m`, `wal-m`, `ant-m`, and `che-m`, then adding Gaussian noisy $\Delta(\mathbf{a}) \sim \mathcal{N}(0, 1)$ to demonstrations with weight $w \in \{0.1, 0.3, 0.6, 0.9\}$ *i.e.*, $\hat{\mathbf{a}} \leftarrow \mathbf{a} + w \cdot \Delta(\mathbf{a})$, and utilize the Gaussian noised action to train our policy, further observing the performance decreasing. As shown in Figure 4. ADR can be well adapt to the demonstrations' noisy. As the noise ratio increases, our method shows only a slight decline in performance on `ant-m`. However, there is no significant drop in performance on other tasks such as `wal-m`, `hop-m`, and `che-m`. Therefore, ADR has a certain level of noise resistance and can still maintain relatively good performance even in the presence of noise within demonstrations.

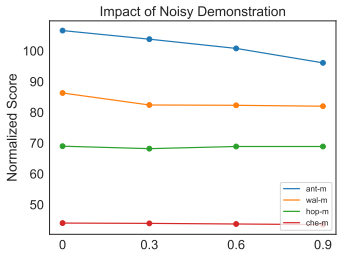

Figure 4: ADR's performance changes as the noise in the demonstrations increases.

Comparison of different methods' OOD risky. To validate our claim that ADR is a supervised in-sample IL approach and therefore does not suffer from overestimation of OOD samples, we compared three different offline algorithms, including CQL (oracle), IQL (oracle), all using the same offline datasets. Specifically, We first trained policies using four different algorithms: ADR, CQL (oracle), IQL (oracle), each with the same datasets. For example, when training ADR with $\mathcal{D}^*$ and $\hat{\mathcal{D}}$, we simultaneously trained CQL (oracle), IQL (oracle) using $\mathcal{D}^* \cup \hat{\mathcal{D}}$. After obtaining the pre-trained models, we sample states from the expert dataset and input them into these pre-trained models. We then plotted heatmaps comparing the logits obtained from these models with the expert policy showing in Figure 5. ADR maintains its decision mode as a demonstration while being less susceptible to OOD scenarios (The more similar the top-left and bottom-right corners of the heatmap are, the closer the algorithm is to the demo).

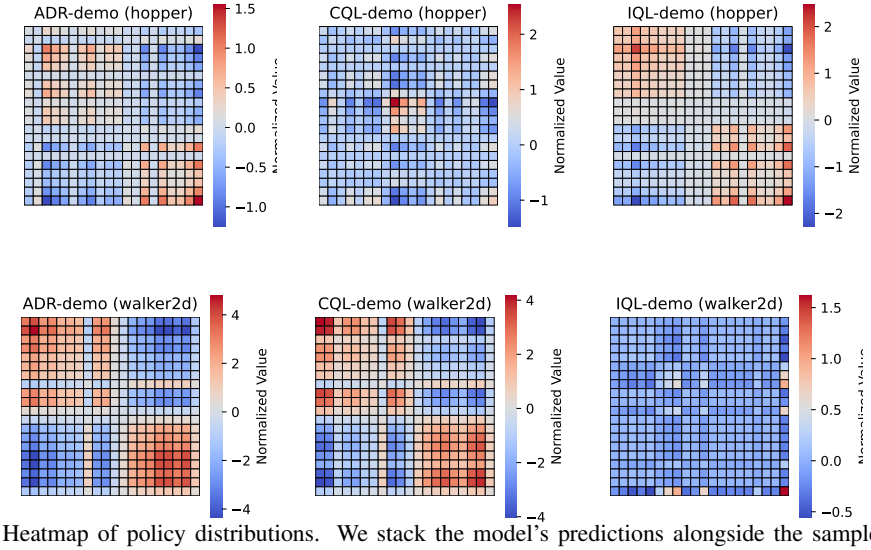

Figure 5: Heatmap of policy distributions. We stack the model's predictions alongside the samples in the dataset. The correlation is higher in the top-left and bottom-right regions, while it is lower in the other areas, the algorithm is less affected by OOD while maintain good performance (details see Appendix F).

8 Conclusion

We proposed ADR, a single-step optimization IL algorithm. Compared to traditional IL algorithms, ADR has two key advantages. First, ADR is a single-step update algorithm, and our theoretical proof shows that minimizing the ADR optimization objective is equivalent to obtaining the optimal policy, resulting in more stable training process. The second advantage is that ADR does not involve modeling the reward or value functions, so it is not affected by sub-optimal value or reward functions. To validate ADR's experimental performance, we tested it on tasks from various tasks in Android and Gym, where ADR outperformed our selected baselines.

REFERENCES

Anthony Brohan, Noah Brown, Justice Carbajal, Yevgen Chebotar, Joseph Dabis, Chelsea Finn, Keerthana Gopalakrishnan, Karol Hausman, Alex Herzog, Jasmine Hsu, Julian Ibarz, Brian Ichter, Alex Irpan, Tomas Jackson, Sally Jesmonth, Nikhil J Joshi, Ryan Julian, Dmitry Kalashnikov, Yuheng Kuang, Isabel Leal, Kuang-Huei Lee, Sergey Levine, Yao Lu, Utsav Malla, Deeksha Manjunath, Igor Mordatch, Ofir Nachum, Carolina Parada, Jodilyn Peralta, Emily Perez, Karl Pertsch, Jornell Quiambao, Kanishka Rao, Michael Ryoo, Grecia Salazar, Pannag Sanketi, Kevin Sayed, Jaspiar Singh, Sumedh Sontakke, Austin Stone, Clayton Tan, Huong Tran, Vincent Vanhoucke, Steve Vega, Quan Vuong, Fei Xia, Ted Xiao, Peng Xu, Sichun Xu, Tianhe Yu, and Brianna Zitkovich. Rt-1: Robotics transformer for real-world control at scale. *arXiv preprint arXiv:2212.06817*, 2023a.

Anthony Brohan, Noah Brown, Justice Carbajal, and etc. Rt-2: Vision-language-action models transfer web knowledge to robotic control. *arXiv preprint arXiv:2307.15818*, 2023b.

Aarushi Bhargava, Vamsi C. Meesala, Muhammad R. Hajj, and Shima Shahab. Nonlinear effects in high-intensity focused ultrasound power transfer systems. *arXiv preprint arXiv:2006.12691*, 2020.

Long Ouyang, Jeff Wu, Xu Jiang, Diogo Almeida, Carroll L. Wainwright, Pamela Mishkin, Chong Zhang, Sandhini Agarwal, Katarina Slama, Alex Ray, John Schulman, Jacob Hilton, Fraser Kelton, Luke Miller, Maddie Simens, Amanda Askell, Peter Welinder, Paul Christiano, Jan Leike, and Ryan Lowe. Training language models to follow instructions with human feedback. *arXiv preprint arXiv:2203.02155*, 2022.

Hugo Touvron, Louis Martin, Kevin Stone, Peter Albert, Amjad Almahairi, Yasmine Babaei, Nikolay Bashlykov, Soumya Batra, Prajjwal Bhargava, Shruti Bhosale, Dan Bikel, Lukas Blecher, Cristian Canton Ferrer, Moya Chen, Guillem Cucurull, David Esiobu, Jude Fernandes, Jeremy Fu, Wenyin Fu, Brian Fuller, Cynthia Gao, Vedanuj Goswami, Naman Goyal, Anthony Hartshorn, Saghar Hosseini, Rui Hou, Hakan Inan, Marcin Kardas, Viktor Kerkez, Madian Khabsa, Isabel Kloumann, Artem Korenev, Punit Singh Koura, Marie-Anne Lachaux, Thibaut Lavril, Jenya Lee, Diana Liskovich, Yinghai Lu, Yuning Mao, Xavier Martinet, Todor Mihaylov, Pushkar Mishra, Igor Molybog, Yixin Nie, Andrew Poulton, Jeremy Reizenstein, Rashi Rungta, Kalyan Saladi, Alan Schelten, Ruan Silva, Eric Michael Smith, Ranjan Subramanian, Xiaoqing Ellen Tan, Binh Tang, Ross Taylor, Adina Williams, Jian Xiang Kuan, Puxin Xu, Zheng Yan, Iliyan Zarov, Yuchen Zhang, Angela Fan, Melanie Kambadur, Sharan Narang, Aurelien Rodriguez, Robert Stojnic, Sergey Edunov, and Thomas Scialom. Llama 2: Open foundation and fine-tuned chat models. 2023.

Rafael Gómez-Bombarelli, Jennifer N Wei, David Duvenaud, José Miguel Hernández-Lobato, Benjamín Sánchez-Lengeling, Dennis Sheberla, Jorge Aguilera-Iparraguirre, Timothy D Hirzel, Ryan P Adams, and Alán Aspuru-Guzik. Automatic chemical design using a data-driven continuous representation of molecules. *ACS central science*, 4(2):268–276, 2018.

Sergey Levine, Aviral Kumar, George Tucker, and Justin Fu. Offline reinforcement learning: Tutorial, review, and perspectives on open problems. *arXiv preprint arXiv:2005.01643*, 2020.

Scott Fujimoto, David Meger, and Doina Precup. Off-policy deep reinforcement learning without exploration. In Kamalika Chaudhuri and Ruslan Salakhutdinov, editors, *Proceedings of the 36th International Conference on Machine Learning*, volume 97 of *Proceedings of Machine Learning Research*, pages 2052–2062. PMLR, 09–15 Jun 2019a. URL https://proceedings.mlr.press/v97/fujimoto19a.html.

Jialong Wu, Haixu Wu, Zihan Qiu, Jianmin Wang, and Mingsheng Long. Supported policy optimization for offline reinforcement learning. *arXiv preprint arXiv:2202.06239*, 2022.

Aviral Kumar, Aurick Zhou, George Tucker, and Sergey Levine. Conservative q-learning for offline reinforcement learning. In H. Larochelle, M. Ranzato, R. Hadsell, M.F. Balcan, and H. Lin, editors, *Advances in Neural Information Processing Systems*, volume 33, pages 1179–1191. Curran Associates, Inc., 2020a. URL https://proceedings.neurips.cc/paper_files/paper/2020/file/0d2b2061826a5df3221116a5085a6052-Paper.pdf.

Zhepeng Cen, Zuxin Liu, Zitong Wang, Yihang Yao, Henry Lam, and Ding Zhao. Learning from sparse offline datasets via conservative density estimation. *arXiv preprint arXiv:2401.08819*, 2024.

Brenna D. Argall, Sonia Chernova, Manuela Veloso, and Brett Browning. A survey of robot learning from demonstration. *Robotics and Autonomous Systems*, 57(5):469–483, 2009. ISSN 0921-8890. doi: https://doi.org/10.1016/j.robot.2008.10.024. URL https://www.sciencedirect.com/science/article/pii/S0921889008001772.

Jonathan Ho and Stefano Ermon. Generative adversarial imitation learning. *arXiv preprint arXiv:1606.03476*, 2016.

Ilya Kostrikov, Ofir Nachum, and Jonathan Tompson. Imitation learning via off-policy distribution matching. *arXiv preprint arXiv:1912.05032*, 2019.

Geon-Hyeong Kim, Seokin Seo, Jongmin Lee, Wonseok Jeon, HyeongJoo Hwang, Hongseok Yang, and Kee-Eung Kim. DemoDICE: Offline imitation learning with supplementary imperfect demonstrations. In *International Conference on Learning Representations*, 2022. URL https://openreview.net/forum?id=BrPdX1bDZkQ.

Yecheng Jason Ma, Andrew Shen, Dinesh Jayaraman, and Osbert Bastani. Versatile offline imitation from observations and examples via regularized state-occupancy matching. *arXiv preprint arXiv:2202.02433*, 2022a.

Siddharth Reddy, Anca D. Dragan, and Sergey Levine. Sqil: Imitation learning via reinforcement learning with sparse rewards. *arXiv preprint arXiv:1905.11108*, 2019.

Aviral Kumar, Justin Fu, George Tucker, and Sergey Levine. Stabilizing off-policy q-learning via bootstrapping error reduction. *arXiv preprint arXiv:1906.00949*, 2019.

Ilya Kostrikov, Ashvin Nair, and Sergey Levine. Offline reinforcement learning with implicit q-learning. *arXiv preprint arXiv:2110.06169*, 2021.

Tuomas Haarnoja, Aurick Zhou, Pieter Abbeel, and Sergey Levine. Soft actor-critic: Off-policy maximum entropy deep reinforcement learning with a stochastic actor. *arXiv preprint arXiv:1801.01290*, 2018a.

Scott Fujimoto, David Meger, and Doina Precup. Off-policy deep reinforcement learning without exploration. *arXiv preprint arXiv:1812.02900*, 2019b.

Hado van Hasselt, Arthur Guez, and David Silver. Deep reinforcement learning with double q-learning. *arXiv preprint arXiv:1509.06461*, 2015.

Stephane Ross, Geoffrey J. Gordon, and J. Andrew Bagnell. A reduction of imitation learning and structured prediction to no-regret online learning, 2011a.

Kshitij Judah, Alan Fern, Prasad Tadepalli, and Robby Goetschalckx. Imitation learning with demonstrations and shaping rewards. *Proceedings of the AAAI Conference on Artificial Intelligence*, 28(1), Jun. 2014. doi: 10.1609/aaai.v28i1.9024. URL https://ojs.aaai.org/index.php/AAAI/article/view/9024.

Daniel S. Brown, Wonjoon Goo, and Scott Niekum. Better-than-demonstrator imitation learning via automatically-ranked demonstrations. In Leslie Pack Kaelbling, Danica Kragic, and Komei Sugiura, editors, *Proceedings of the Conference on Robot Learning*, volume 100 of *Proceedings of Machine Learning Research*, pages 330–359. PMLR, 30 Oct–01 Nov 2020. URL https://proceedings.mlr.press/v100/brown20a.html.

Harish Ravichandar, Athanasios S. Polydoros, Sonia Chernova, and Aude Billard. Recent advances in robot learning from demonstration. *Annual Review of Control, Robotics, and Autonomous Systems*, 3(1):297–330, 2020. doi: 10.1146/annurev-control-100819-063206. URL https://doi.org/10.1146/annurev-control-100819-063206.

Damian Boborzi, Christoph-Nikolas Straehle, Jens S. Buchner, and Lars Mikelsons. Imitation learning by state-only distribution matching. *arXiv preprint arXiv:2202.04332*, 2022.

Stephane Ross, Geoffrey Gordon, and Drew Bagnell. A reduction of imitation learning and structured prediction to no-regret online learning. In Geoffrey Gordon, David Dunson, and Miroslav Dudík, editors, *Proceedings of the Fourteenth International Conference on Artificial Intelligence and Statistics*, volume 15 of *Proceedings of Machine Learning Research*, pages 627–635, Fort Lauderdale, FL, USA, 11–13 Apr 2011b. PMLR. URL https://proceedings.mlr.press/v15/ross11a.html.

YuXuan Liu, Abhishek Gupta, Pieter Abbeel, and Sergey Levine. Imitation from observation: Learning to imitate behaviors from raw video via context translation. In *2018 IEEE International Conference on Robotics and Automation (ICRA)*, pages 1118–1125, 2018. doi: 10.1109/ICRA.2018.8462901.

Faraz Torabi, Garrett Warnell, and Peter Stone. Recent advances in imitation learning from observation. *arXiv preprint arXiv:1905.13566*, 2019.

Jinxin Liu, Li He, Yachen Kang, Zifeng Zhuang, Donglin Wang, and Huazhe Xu. Ceil: Generalized contextual imitation learning. *arXiv preprint arXiv:2306.14534*, 2023a.

Ziqi Zhang, Jingzehua Xu, Jinxin Liu, Zifeng Zhuang, and Donglin Wang. Context-former: Stitching via latent conditioned sequence modeling. *arXiv preprint arXiv:2401.16452*, 2024.

Yifan Wu, George Tucker, and Ofir Nachum. Behavior regularized offline reinforcement learning. *arXiv preprint arXiv:1911.11361*, 2019.

Diederik P Kingma and Max Welling. Auto-encoding variational bayes. *arXiv preprint arXiv:1312.6114*, 2022.

Mohamed Debbagh. Learning structured output representations from attributes using deep conditional generative models. *arXiv preprint arXiv:2305.00980*, 2023.

Mathieu Germain, Karol Gregor, Iain Murray, and Hugo Larochelle. Made: Masked autoencoder for distribution estimation. *arXiv preprint arXiv:1502.03509*, 2015.

Scott Fujimoto and Shixiang Shane Gu. A minimalist approach to offline reinforcement learning. *arXiv preprint arXiv:2106.06860*, 2021.

Ashvin Nair, Abhishek Gupta, Murtaza Dalal, and Sergey Levine. Awac: Accelerating online reinforcement learning with offline datasets. *arXiv preprint arXiv:2006.09359*, 2021.

Simon Damm, Dennis Forster, Dmytro Velychko, Zhenwen Dai, Asja Fischer, and Jörg Lücke. The elbo of variational autoencoders converges to a sum of three entropies. *arXiv preprint arXiv:2010.14860*, 2023.

Andrei A. Rusu, Sergio Gomez Colmenarejo, Caglar Gulcehre, Guillaume Desjardins, James Kirkpatrick, Razvan Pascanu, Volodymyr Mnih, Koray Kavukcuoglu, and Raia Hadsell. Policy distillation. *arXiv preprint arXiv:1511.06295*, 2016.

Aaron van den Oord, Oriol Vinyals, and Koray Kavukcuoglu. Neural discrete representation learning. *arXiv preprint arXiv:1711.00937*, 2018.

Justin Fu, Aviral Kumar, Ofir Nachum, George Tucker, and Sergey Levine. D4rl: Datasets for deep data-driven reinforcement learning. *arXiv preprint arXiv:2004.07219*, 2021.

Yicheng Luo, Zhengyao Jiang, Samuel Cohen, Edward Grefenstette, and Marc Peter Deisenroth. Optimal transport for offline imitation learning. *arXiv preprint arXiv:2303.13971*, 2023.

Jinxin Liu, Lipeng Zu, Li He, and Donglin Wang. Clue: Calibrated latent guidance for offline reinforcement learning. *arXiv preprint arXiv:2306.13412*, 2023b.

Divyansh Garg, Shuvam Chakraborty, Chris Cundy, Jiaming Song, Matthieu Geist, and Stefano Ermon. Iq-learn: Inverse soft-q learning for imitation. *arXiv preprint arXiv:2106.12142*, 2022.

Tuomas Haarnoja, Aurick Zhou, Pieter Abbeel, and Sergey Levine. Soft actor-critic: Off-policy maximum entropy deep reinforcement learning with a stochastic actor. *arXiv preprint arXiv:1801.01290*, 2018b. URL https://arxiv.org/abs/1801.01290.

Konrad Zolna, Alexander Novikov, Ksenia Konyushkova, Caglar Gulcehre, Ziyu Wang, Yusuf Aytar, Misha Denil, Nando de Freitas, and Scott Reed. Offline learning from demonstrations and unlabeled experience. *arXiv preprint arXiv:2011.13885*, 2020.

Fumihiro Sasaki and Ryota Yamashina. Behavioral cloning from noisy demonstrations. In *International Conference on Learning Representations*, 2021. URL https://openreview.net/forum?id=zrT3HcsWSAt.

Aviral Kumar, Aurick Zhou, George Tucker, and Sergey Levine. Conservative q-learning for offline reinforcement learning. *arXiv preprint arXiv:2006.04779*, 2020b.

Rishabh Agarwal, Max Schwarzer, Pablo Samuel Castro, Aaron Courville, and Marc G. Bellemare. Deep reinforcement learning at the edge of the statistical precipice. *arXiv preprint arXiv:2108.13264*, 2022.

Lili Chen, Kevin Lu, Aravind Rajeswaran, Kimin Lee, Aditya Grover, Michael Laskin, Pieter Abbeel, Aravind Srinivas, and Igor Mordatch. Decision transformer: Reinforcement learning via sequence modeling. *arXiv preprint arXiv:2106.01345*, 2021.

Denis Tarasov, Alexander Nikulin, Dmitry Akimov, Vladislav Kurenkov, and Sergey Kolesnikov. CORL: Research-oriented deep offline reinforcement learning library. In *3rd Offline RL Workshop: Offline RL as a "Launchpad"*, 2022. URL https://openreview.net/forum?id=SyAS49bBcv.

Yecheng Jason Ma, Andrew Shen, Dinesh Jayaraman, and Osbert Bastani. Versatile offline imitation from observations and examples via regularized state-occupancy matching. *arXiv preprint arXiv:2202.02433*, 2022b.

CONTENTS

1 Introduction **1**

2 Related Work **2**

3 Preliminaries **3**

4 Problem Formulation **4**

5 Theoretical Analysis of Adversarial Density Regression **5**

6 Methods **6**

6.1 Practical Implementation 7

7 Evaluation **7**

7.1 Majority experimental results 8

7.2 Ablations 9

8 Conclusion **10**

A Limitations **16**

B Social Impacts **16**

C Hyper parameters and Implementation details **16**

D Theoretical Analysis **17**

E Experimental results of baselines **20**

F Evaluation Details **20**

A LIMITATIONS

We have currently attempted to extend ADR to sequential models, such as the Decision Transformer (DT) (Chen et al., 2021) (Remove the Return token and use transformer as a fully supervised policy), but we have found that the experimental results are not as impressive as those under the MDP setting. We will further explore the possibility of extending ADR to sequential models.

B SOCIAL IMPACTS

We propose a new supervised iIL framework, ADR. Meanwhile, we point out that the advantage of ADR lies in that it can effectively avoid the cumulative offset sourced from sub-optimal Reward/Value function. Besides we In addition, the effect of ADR exceeds all previous imitation learning frameworks and even achieves better performance than IQL on robotic arm/kitchen tasks, which will greatly promote the development of imitation learning frameworks under supervised learning.

C HYPER PARAMETERS AND IMPLEMENTATION DETAILS

Our method is slightly dependent on hyper-parameters. We introduce the core hyperparameters here:

Table 4: Crucial hyper-parameters of ADR.

Hyperparameter	Value
VAE training iterations	$1e^5$
policy training iterations	$1e^6$
batch size	64
learning rate (lr) of π	$1e^{-4}$
lr of VQ-VAE	$1e^{-3}$
evaluation frequency	$1e^3$
L in Equation 6	1
λ in Equation 16	1
Optimizing Equation 12	All selected tasks except for `che-mr`
Random Seeds	{0,2,4,6}
Optimizing Equation 9	`che-mr`
Model Architecture	
MLP Policy	4× Layers MLP (hidden dim 256)
VQVAE (encoder and decoder)	3× Layers MLP (hidden dim: 2× action dim; latent dim: 750) 4096 tabular embeddings

Our code is based on CORL (Tarasov et al., 2022). Specifically, in terms of a training framework, we adapted the offline training framework of Supported Policy Optimization (SPOT) (Wu et al., 2022), decomposing it into multiple modules and modifying it to implement our algorithm. Regarding the model architecture, we implemented the VQVAE ourselves, while the MLP policy architecture is based on CORL. Some general details such as warm-up, a discount of lr, *e.g.*, are implemented by CORL. *We have appended our source code in the supplement materials.*

Computing efficiency of DWR. To further showcase the computational efficiency of DWR, we selected the `che-mr` environment as the benchmark and systematically varied the batch size from 10 to 300 while measuring the training time (using a 1000-step size in the policy updating stage). As depicted in Figure 6, it's evident that the training time of ADR is significantly lower compared to ADE-divergence (which shares the same conceptual framework as Equation 8), and such advantage becomes especially pronounced with larger batch sizes. Therefore, the computational efficiency of ADR has been convincingly demonstrated.

Ablation of the upper bound of ADR. In order to demonstrate the effectiveness of minimizing Equation 12 (upper-bound) over minimizing Equation 9 (objective), we conduct fine-grained com-

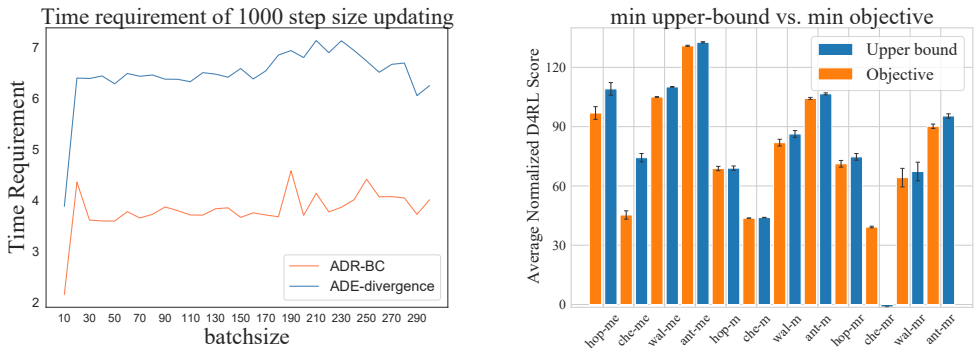

Figure 6: (Left) Comparison of training time. (Right) Abaltion of upper bound.

parisons. Specifically, we compare minimizing Equation 12, Equation 9 on all selected tasks sourced from Gym-Mujoco domain (hop denotes hopper, wal denotes walker2d, che denotes halfcheetah), minimizing Equation 12 achieve overall better performance (8 out of 12), indicating the necessity of Equation 12.

D THEORETICAL ANALYSIS

Theorem D.1 (Density Weight). *Given expert log behavior density* $\log P^*(\mathbf{a}|\mathbf{s}) : \mathcal{S} \times \mathcal{A} \to \mathbb{R}$*, sub-optimal log behavior density* $\log \hat{P}(\mathbf{a}|\mathbf{s}) : \mathcal{S} \times \mathcal{A} \to \mathbb{R}$*, and the empirical policy* $\pi_\theta : \mathcal{S} \to \mathcal{A}$*, offline dataset* $\mathcal{D}$*. Minimizing the KL divergence between* π_θ *and* P^**, while maximizing the KL divergence between* π_θ *and* $\hat{P}$*, i.e., Equation 8. is equivalent to:* $\min_{\pi_\theta} \mathbb{E}_{(\mathbf{s},\mathbf{a})\sim\mathcal{D}}\big[\log \frac{P^*(\mathbf{a}|\mathbf{s})}{\hat{P}(\mathbf{a}|\mathbf{s})} \cdot ||\pi_\theta(\cdot|\mathbf{s}) - \mathbf{a}||_2\big]$,

Proof

$$
\begin{aligned}
J(\pi_\theta) &= \mathbb{E}_{(\mathbf{s},\mathbf{a})\sim\mathcal{D}}[D_{\mathrm{KL}}[\pi_\theta||P^*] - D_{\mathrm{KL}}[\pi_\theta||\hat{P}]] \\
&= \mathbb{E}_{(\mathbf{s},\mathbf{a})\sim\mathcal{D}}\left[\pi_\theta(\mathbf{a}|\mathbf{s}) \cdot \log \frac{\pi_\theta(\mathbf{a}|\mathbf{s})}{P^*(\mathbf{a}|\mathbf{s})}\right] - \mathbb{E}_{(\mathbf{s},\mathbf{a})\sim\mathcal{D}}\left[\pi_\theta(\mathbf{a}|\mathbf{s}) \cdot \log \frac{\pi_\theta(\mathbf{a}|\mathbf{s})}{\hat{P}(\mathbf{a}|\mathbf{s})}\right] \\
&= \mathbb{E}_{(\mathbf{s},\mathbf{a})\sim\mathcal{D}}\left[\pi_\theta(\mathbf{a}|\mathbf{s}) \cdot \left(\log \frac{\pi_\theta(\mathbf{a}|\mathbf{s})}{P^*(\mathbf{a}|\mathbf{s})} - \log \frac{\pi_\theta(\mathbf{a}|\mathbf{s})}{\hat{P}(\mathbf{a}|\mathbf{s})}\right)\right] \\
&= \mathbb{E}_{(\mathbf{s},\mathbf{a})\sim\mathcal{D}}\big[\pi_\theta(\mathbf{a}|\mathbf{s}) \cdot \log \frac{\hat{P}(\mathbf{a}|\mathbf{s})}{P^*(\mathbf{a}|\mathbf{s})}\big] \\
&= \mathbb{E}_{(\mathbf{s},\mathbf{a})\sim\mathcal{D}}\big[\mathcal{W}(\hat{P}, P^*) \cdot \pi_\theta(\mathbf{a}|\mathbf{s})\big] \\
&\overset{\text{def}}{=} \mathbb{E}_{(\mathbf{s},\mathbf{a})\sim\mathcal{D}}\big[\mathcal{W}(\hat{P}, P^*) \cdot ||\pi_\theta(\cdot|\mathbf{s}) - \mathbf{a}||^2\big]
\end{aligned}
\tag{18}
$$

Assumption D.2. *Assuming* $D_{KL}[\pi^*||\hat{\pi}] \leq \delta$

Theorem D.3. *Given* $\mathcal{D}^*$*, based on Assumption D.2, we have:*

$$
\mathbb{E}_{\mathcal{D}^*}[\pi^* \log \frac{\pi^*}{\hat{\pi}}] \leq \frac{M}{2n} \cdot \sqrt{\log \frac{2}{\delta}} \tag{19}
$$

with probability $1 - \delta$*. Where* $n = |\mathcal{D}^*|$*,* $M = \max_{(\mathbf{s}_t,\mathbf{a}_t)} \pi^*(\mathbf{a}_t|\mathbf{s}_t) \log \frac{\pi^*(\mathbf{a}_t|\mathbf{s}_t)}{\hat{\pi}(\mathbf{a}|\mathbf{s})}|_{(\mathbf{s}_t,\mathbf{a}_t)\sim\mathcal{D}^*}$

Proof

Our derivation is based on Hoeffding in-equality, and We first let $X_i = \pi^*(\mathbf{a}_i|\mathbf{s}_i) \log \frac{\pi^*(\mathbf{a}_i|\mathbf{s}_i)}{\hat{\pi}(\mathbf{a}|\mathbf{s})}$, $\bar{X} = \frac{\sum_t X_t}{n}$, then we have:

$$
P(|\bar{X}_i - \mathbb{E}_{\pi^*}[D_{KL}[\pi||\pi^*]]| \geq m) \leq 2 \cdot e^{-\frac{2n^2 \cdot m^2}{M^2}} \tag{20}
$$

Then let $2 \cdot e^{-\frac{2n^2 \cdot m^2}{M^2}} = \delta$, we obtain $t = \frac{M}{2n}\sqrt{\log \frac{2}{\delta}}$. Furthermore, with $1-\delta$ probability we have:

$$|\bar{X}_i - \mathbb{E}_{\pi^*}[D_{KL}[\pi||\pi^*]]| \leq 2 \cdot e^{-\frac{2n^2 \cdot m^2}{M^2}} \tag{21}$$

Meanwhile, we have assumed that $D_{KL}[\pi^*||\hat{\pi}] \leq \delta$, and thus we obtain $\mathbb{E}_{\mathcal{D}^*}[\pi^* \log \frac{\pi^*}{\hat{\pi}}] \leq \frac{M}{2n} \cdot \sqrt{\log \frac{2}{\delta}}$

Proposition D.4 (Policy Convergence of ADR)**.** *Assuming Equation 8 can finally converge to ϵ via minimizing Eq 10, meanwhile, assuming Assumption D.2 is held. Then $\mathbb{E}_{(\mathbf{s},\mathbf{a})\sim\hat{\mathcal{D}}}[D_{KL}(\pi||\pi^*)] \rightarrow \frac{M}{2n} \cdot \sqrt{\log \frac{2}{\delta}} + \Delta C + \epsilon$.Where $n = |\mathcal{D}^*|, M := \arg\max_{X_i}\{X_i = \pi^*(\mathbf{a}_t|\mathbf{s}_t) \log \frac{\pi^*(\mathbf{a}_t|\mathbf{s}_t)}{\hat{\pi}(\mathbf{a}_t|\mathbf{s}_t)} | (\mathbf{s}_t, \mathbf{a}_t) \sim \mathcal{D}^*\}$ with probability $1-\delta$.*

Proof

Using Bayes' rule, we have: $P^*(\mathbf{a}|\mathbf{s}) = \frac{\pi^*(\mathbf{a}|\mathbf{s})P(\mathbf{s})}{P^*(\mathbf{s})}, \quad \hat{P}(\mathbf{a}|\mathbf{s}) = \frac{\hat{\pi}(\mathbf{a}|\mathbf{s})P(\mathbf{s})}{\hat{P}(\mathbf{s})}$

Substitute it into the KL divergence terms in the objective function.$D_{KL}[\pi||P^*]$, $D_{KL}[\pi||\hat{P}]$, we have

$$\mathbb{E}_{\mathcal{D}}[D_{KL}[\pi||P^*]] = \mathbb{E}_{\mathcal{D}}\left[\pi(\mathbf{a}|\mathbf{s}) \cdot \log \frac{\pi(\mathbf{a}|\mathbf{s})}{P^*(\mathbf{a}|\mathbf{s})}\right] = \mathbb{E}_{\mathcal{D}}\left[D_{KL}[\pi||\pi^*]\right] + C_1 \tag{22}$$

$$\mathbb{E}_{\mathcal{D}}[D_{KL}[\pi||\hat{P}]] = \mathbb{E}_{\mathcal{D}}\left[\pi(\mathbf{a}|\mathbf{s}) \cdot \log \frac{\pi(\mathbf{a}|\mathbf{s})}{\hat{P}(\mathbf{a}|\mathbf{s})}\right] = \mathbb{E}_{\mathcal{D}}\left[D_{KL}[\pi||\hat{\pi}]\right] + C_2 \tag{23}$$

Here, C_1 and C_2 are constants related to the marginal distribution of the state $P(s)$, $\hat{P}(s)$ and $P^*(s)$, and they do not change with the policy π

Then, we bring Equation 22 and Equation 23 to Equation 8. Then we have

$$\mathbb{E}_{\mathcal{D}}\left[D_{KL}[\pi||\pi^*]\right] + C_1 - \left(\mathbb{E}_{\mathcal{D}}\left[D_{KL}[\pi||\hat{\pi}]\right] + C_2\right) \leq \epsilon \tag{24}$$

Case 1 Meanwhile, we can observe from Equation D.1 that it's a weighted BC objective, and we assume this objective can well estimate the offline dataset *i.e.*, $\mathbb{E}_{\hat{\mathcal{D}}}[D_{KL}[\pi||\hat{\pi}]] \rightarrow 0$, therefore $\mathbb{E}_{\mathcal{D}}[D_{KL}[\pi||\hat{\pi}]] = \mathbb{E}_{\hat{\mathcal{D}}\cup\mathcal{D}^*}[D_{KL}[\pi||\hat{\pi}]] \approx \mathbb{E}_{\hat{\mathcal{D}}}[D_{KL}[\pi||\hat{\pi}]]$.

Case 2 Similar to **Case 1**, we can also obtain: $\mathbb{E}_{\mathcal{D}^*}[D_{KL}[\pi||\hat{\pi}]] \approx \mathbb{E}_{\mathcal{D}^*}[D_{KL}[\pi^*||\hat{\pi}]]]$.

Assign Equation 24, we have

$$\mathbb{E}_{\mathcal{D}}\left[D_{KL}[\pi||\pi^*]\right] - \mathbb{E}_{\mathcal{D}}\left[D_{KL}[\pi||\hat{\pi}]\right] \leq \epsilon + C_2 - C_1 \tag{25}$$

$$\textbf{(Pinsker's in-equality)}\ \mathbb{E}_{\mathcal{D}}\left[D_{KL}[\pi||\pi^*]\right] \leq \mathbb{E}_{\mathcal{D}}\left[D_{KL}[\pi||\hat{\pi}]\right] + \Delta C + \epsilon \tag{26}$$

$$(\textbf{Case 1})\ \mathbb{E}_{\mathcal{D}}\left[D_{KL}[\pi||\pi^*]\right] \leq \mathbb{E}_{\mathcal{D}^*}\left[D_{KL}[\pi||\hat{\pi}]\right] + \Delta C + \epsilon \tag{27}$$

$$(\textbf{Case 2})\ \mathbb{E}_{\mathcal{D}}\left[D_{KL}[\pi||\pi^*]\right] \leq \mathbb{E}_{\mathcal{D}^*}\left[D_{KL}[\pi^*||\hat{\pi}]\right] + \Delta C + \epsilon \tag{28}$$

$$(\textbf{Theorem D.3})\ \mathbb{E}_{\mathcal{D}}\left[D_{KL}[\pi||\pi^*]\right] \leq \frac{M}{2n} \cdot \sqrt{\log \frac{2}{\delta}} + \Delta C + \epsilon, \tag{29}$$

where, $\Delta C = C_1 - C_2$ is a constant term, dependent on the state distribution. δ originates from Assumption D.2, $n = |\mathcal{D}^*|$, $M := \arg\max_{X_i}\{X_i = \pi^*(\mathbf{a}_t|\mathbf{s}_t) \log \frac{\pi^*(\mathbf{a}_t|\mathbf{s}_t)}{\hat{\pi}(\mathbf{a}_t|\mathbf{s}_t)} | (\mathbf{s}_t, \mathbf{a}_t) \sim \mathcal{D}^*\}$.

Lemma D.5. *Given the state distribution of empirical and expert policy $d(\mathbf{s})$, $d^{\pi^*}(\mathbf{s})$. Meanwhile, given the state-action distribution of empirical and expert policy $d^{\pi}(\mathbf{s},\mathbf{a})$, $d^{\pi^*}(\mathbf{s},\mathbf{a})$ we have:*

$$D_{KL}[d^{\pi}(\mathbf{s})||d^{\pi^*}(\mathbf{s})] \leq D_{KL}[d^{\pi}(\mathbf{s},\mathbf{a})||d^{\pi^*}(\mathbf{s},\mathbf{a})] \tag{30}$$

Lemma D.6. *Given the distribution of empirical and expert transitions $d^{\pi}(\mathbf{s},\mathbf{a},\mathbf{s}')$, $d^{\pi^*}(\mathbf{s},\mathbf{a},\mathbf{s}')$ we have following relationship:*

$$D_{KL}[d^{\pi}(\mathbf{s},\mathbf{a},\mathbf{s}')||d^{\pi^*}(\mathbf{s},\mathbf{a},\mathbf{s}')] = D_{KL}[d^{\pi}(\mathbf{s},\mathbf{a})||d^{\pi^*}(\mathbf{s},\mathbf{a})] \tag{31}$$

Proof of Lemma D.5 and Lemma D.6 see Lemma 1 and Lemma 2 from Ma et al.

Assumption D.7. *Suppose the policy extracted from Equation is π, we separately define the state marginal of the dataset, empirical policy, and expert policy as $d^{\mathcal{D}}$, d^{π} and d^{π^*}, they satisfy this relationship:*

$$D_{KL}[d^{\pi}||d^{\pi^*}] \leq D_{KL}[d^{\mathcal{D}}||d^{\pi^*}] \tag{32}$$

Lemma D.8 (lemma 2 from Cen et al. (2024))**.** *Suppose the maximum reward is $R_{max} = \max||r(\mathbf{s},\mathbf{a})||$, and $V(\rho_0) = \mathbb{E}_{\mathbf{s}_0}[V(\mathbf{s}_0)]$ denote the performance given a policy π, then with Assumption D.7:*

$$|V^{\pi}(\rho_0) - V^{\pi^*}(\rho_0)| \leq \frac{R_{max}}{1-\gamma} D_{TV}[d^*(\mathbf{s})||d^{\mathcal{D}}(\mathbf{s})] + \frac{2\cdot R_{max}}{1-\gamma} E_{d^{\mathcal{D}}}[D_{TV}[\pi(\cdot|\mathbf{s})||\pi^*(\cdot||\mathbf{s})]] \tag{33}$$

Proof of Lemma D.8 see Lemma 2 from Cen et al.

Proposition D.9. *(Value Bound of ADR) Given the empirical policy π and the optimal policy π^*, let $V^{\pi}(\rho_0)$ and $V^{\pi^*}(\rho_0)$ separately denote the value network of π and π^*, and given the discount factor γ. Meanwhile, let R_{max} as the upper bound of the reward function i.e., $R_{max} = \max||r(\mathbf{s},\mathbf{a})||$. Based on the Assumption D.7, Assumption D.2, Lemma D.8, and Proposition 5.2, we can obtain:*

$$|V^{\pi}(\rho_0) - V^{\pi^*}(\rho_0)| \leq \frac{R_{max}}{1-\gamma} D_{TV}[d^*(\mathbf{s})||d^{\mathcal{D}}(\mathbf{s})] + \frac{2\cdot R_{max}}{1-\gamma} \cdot \sqrt{2\cdot(\frac{M}{2n}\cdot\sqrt{\log\frac{2}{\delta}} + \Delta C + \epsilon)}, \tag{34}$$

Where, $\Delta C = C_1 - C_2$ is a constant term, typically dependent on the state distribution. The δ originates from Assumption D.2, $n = |\mathcal{D}^*|$, $M := \arg\max_{X_i}\{X_i = \pi^*(\mathbf{a}_t|\mathbf{s}_t)\log\frac{\pi^*(\mathbf{a}_t|\mathbf{s}_t)}{\hat{\pi}(\mathbf{a}_t|\mathbf{s}_t)}|(\mathbf{s}_t,\mathbf{a}_t)\sim\mathcal{D}^*\}$.

Proof

In Proposition 5.2, we have proved that if $\mathbb{E}_{(\mathbf{s},\mathbf{a})\sim\mathcal{D}}\left[\pi_{\theta}(\mathbf{a}|\mathbf{s})\cdot\log\frac{\hat{P}(\mathbf{a}|\mathbf{s})}{P^*(\mathbf{a}|\mathbf{s})}\right]$ can finally converge to ϵ. Then $\mathbb{E}_{(\mathbf{s},\mathbf{a})\sim\hat{\mathcal{D}}}[D_{KL}(\pi||\pi^*)] \to \frac{M}{2n}\cdot\sqrt{\log\frac{2}{\delta}} + \Delta C + \epsilon$

Subsequently, based on Lemma D.8, we derivative:

$$\begin{aligned}
|V^{\pi}(\rho_0) - V^{\pi^*}(\rho_0)| \leq & \frac{R_{max}}{1-\gamma} D_{TV}[d^*(\mathbf{s})||d^{\mathcal{D}}(\mathbf{s})] + \frac{2\cdot R_{max}}{1-\gamma} E_{d^{\mathcal{D}}}[D_{TV}[\pi(\cdot|\mathbf{s})||\pi^*(\cdot||\mathbf{s})]] && (35)\\
\leq & \frac{R_{max}}{1-\gamma} D_{TV}[d^*(\mathbf{s})||d^{\mathcal{D}}(\mathbf{s})] + \frac{2\cdot R_{max}}{1-\gamma} E_{d^{\mathcal{D}}}[\sqrt{2\cdot D_{KL}[\pi(\cdot|\mathbf{s})||\pi^*(\cdot||\mathbf{s})]}] && (36)\\
= & \frac{R_{max}}{1-\gamma} D_{TV}[d^*(\mathbf{s})||d^{\mathcal{D}}(\mathbf{s})] + \frac{2\cdot R_{max}}{1-\gamma} \cdot \sqrt{2\cdot(\frac{M}{2n}\cdot\sqrt{\log\frac{2}{\delta}} + \Delta C + \epsilon)} && (37)
\end{aligned}$$

E EXPERIMENTAL RESULTS OF BASELINES

Our baselines on Gym-Mujoco domain mainly includes: ORIL (Zolna et al., 2020), SQIL (Reddy et al., 2019), IQ-Learn (Garg et al., 2022), ValueDICE (Kostrikov et al., 2019), DemoDICE (Kim et al., 2022), SMODICE (Ma et al., 2022a), and CEIL (Liu et al., 2023a). The majority of experimental results of these baselines are cited from CEIL (Liu et al., 2023a).

In terms of evaluation on kitchen or androits domains. The majority baselines include OTR (Luo et al., 2023) and CLUE (Liu et al., 2023b) that utilize reward estimating via IL approaches, and policy optimization via Implicit Q Learning (IQL) (Kostrikov et al., 2021). We also encompass Conservative Q Learning (CQL) (Kumar et al., 2020b) and IQL for comparison. Specifically, these experimental results are from:

- The experiment results of OTR and CLUE are directly cited from Luo et al. and Liu et al.
- The experimental results of CQL (oracle) and IQL (oracle) are separately cited from Kumar et al. and Kostrikov et al., and the experimental results of OTR on kitchen domain is obtained by running the official codebase `https://github.com/ethanluoyc/optimal_transport_reward`.

F EVALUATION DETAILS

We run each task multiple times, recording all evaluated results and taking the highest score from each run as the outcome. We then average these highest scores. For score computation, we use the same metric as D4rl *i.e.*, $\frac{\text{output}-\text{expert}}{\text{expert}-\text{random}} \times 100$. Our experiment are running on computing clusters with 16×4 core cpu (Intel(R) Xeon(R) CPU E5-2637 v4 @ 3.50GHz), and 16×RTX2080 Ti GPUs

Table 5: Experimental results from All seeds. Includes 5 demonstrations for learning from demonstration (Lfd) on the Gym-mujoco domain, and 1 demonstration for Lfd on the Kitchen and Androits domain. Our seeds are 0, 2, 4, 6. The training data is included in the appendix, and the value of each seed is obtained by returning the maximum value.

Tasks	**Seed 1**	**Seed 2**	**Seed 3**	**Seed 4**	**Avg.**
`hopper-me`	108.73135306	112.36561301	104.13708473	111.21583144	109.1± 3.2
`halfcheetah-me`	76.91686914	73.34520366	71.3600813	75.65439524	74.3± 2.1
`walker2d-me`	110.01480035	110.15162557	110.41349757	109.86814345	110.1± 0.2
`Ant-me`	132.47422373	132.43903581	132.87375784	133.18474616	132.7± 0.3
`hopper-m`	67.43902685	68.53755386	69.49494087	70.39486176	69.0± 1.1
`halfcheetah-m`	44.26977365	43.96688663	43.96063228	44.002488	44.0± 0.1
`walker2d-m`	89.01287452	84.82661744	84.96199657	86.20352661	86.3± 1.7
`Ant-m`	107.18757783	105.82195401	106.37078241	106.89800012	106.6± 0.5
`hopper-mr`	76.28604245	75.62349403	75.23570126	71.8023475	74.7± 1.7
`halfcheetah-mr`	39.04827579	39.08606318	39.24549748	39.34331542	39.2± 0.1
`walker2d-mr`	69.91171614	60.40786853	72.87922707	65.9015982	67.3± 4.7
`Ant-mr`	95.29014082	97.260068	94.74996758	94.31474188	95.4± 1.1
`door-cloned`	3.3699566	4.83888018	4.5226364	6.33812655	4.8± 1.1
`door-human`	9.35201591	13.05773712	9.10674378	18.71432687	12.6± 3.9
`hammer-cloned`	12.26944958	19.06662599	18.08395955	21.09296431	17.6± 3.3
`hammer-human`	9.37490127	13.78847087	40.01083644	23.73657046	21.7± 11.8
`pen-cloned`	110.88785576	92.09658	75.64396931	59.05532153	84.4± 19.2
`pen-human`	118.47072952	136.50561455	107.8325132	119.68575723	120.6± 10.3
`relocate-cloned`	-0.19486202	-0.18540353	-0.25482428	-0.23930115	-0.2± 0.0
`relocate-human`	0.92621742	3.62704217	3.07594114	0.2939339	2.0± 1.4
`kitchen-mixed`	87.5	90.0	87.5	85.0	87.5± 1.8
`kitchen-partial`	80.0	77.5	85.0	80.0	80.6± 2.7
`kitchen-completed`	95.0	-	-	-	95.0

Training stability of ADR. Despite behavior cloning not being theoretically monotonic, we still present the training curve of ADR. As shown in Figure 7 and Figure 8, we averaged multiple runs and plotted the training curve, demonstrating that ADR exhibits stable training performance.

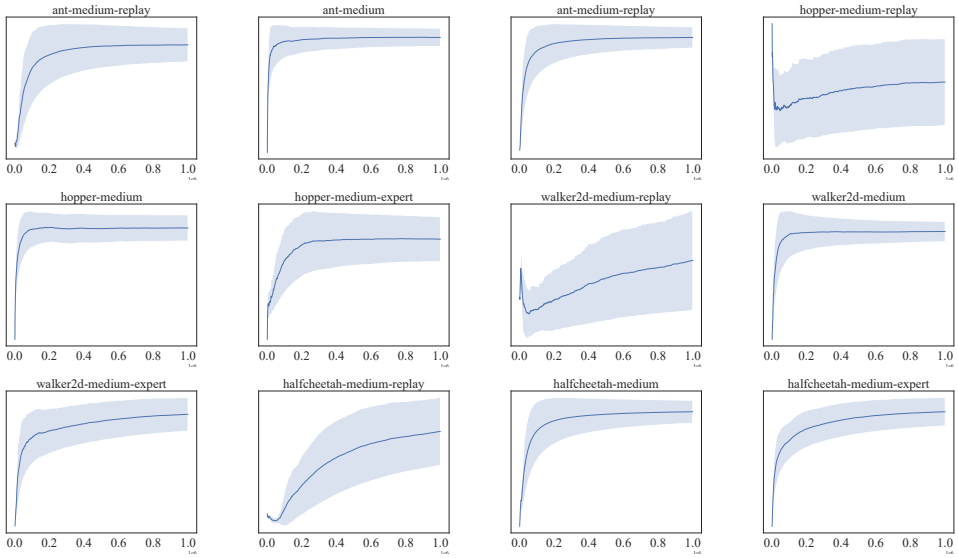

Figure 7: Training curves of ADR on all tasks sourced from Gym-Mujoco domain.

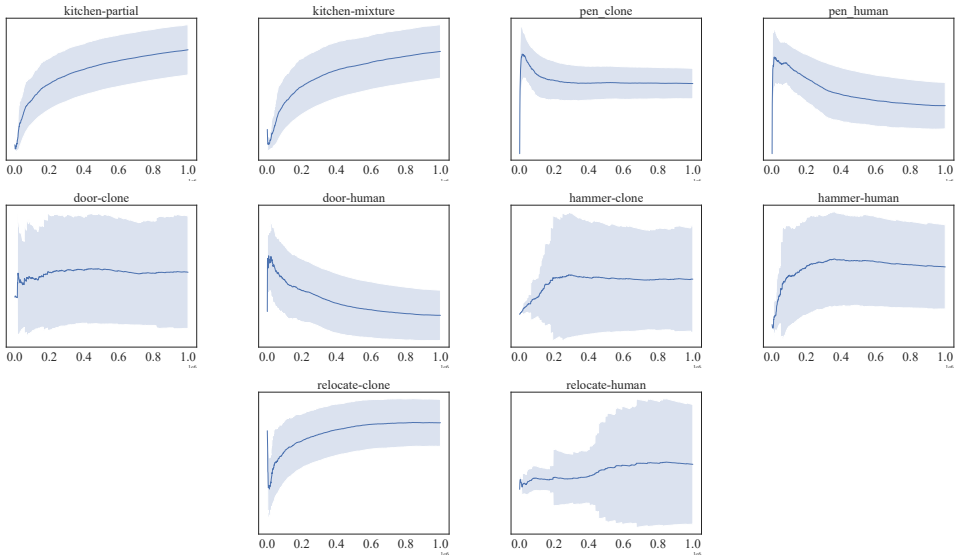

Figure 8: Training curves of ADR on tasks sourced from kitchen and androits domain.

OOD Risky Analysis. We further elaborate on the process of collecting experimental results related to Figure 9. Firstly, we need to train policys on chosen datasets. Specifically, our ADR is trained on five expert trajectories as demonstrations $\mathcal{D}^*$ and the complete medium-replay dataset $\hat{\mathcal{D}}$, which serves as the unknown-quality dataset mentioned in the paper, while retaining the best-performing model. Additionally, when training IQL and CQL, we mix the demonstrations $\mathcal{D}^* \cup \hat{\mathcal{D}}$ with the unknown-quality dataset and use both IQL and CQL algorithms for training. After obtaining the models, we collect the logits from different models using the following specific method: we sample the states $\{\mathbf{s}_{-20}, \mathbf{s}_{-19}, \cdots, \mathbf{s}_{-1}\} \sim \pi^*$ of the last 20 steps from a trajectory in the expert dataset and use them as inputs for ADR, IQL, and CQL. Simultaneously, we retain the actions $\{\mathbf{a}_{-20}, \mathbf{a}_{-19}, \cdots, \mathbf{a}_{-1}\} \sim \pi^*$ corresponding to these states to create heatmaps.

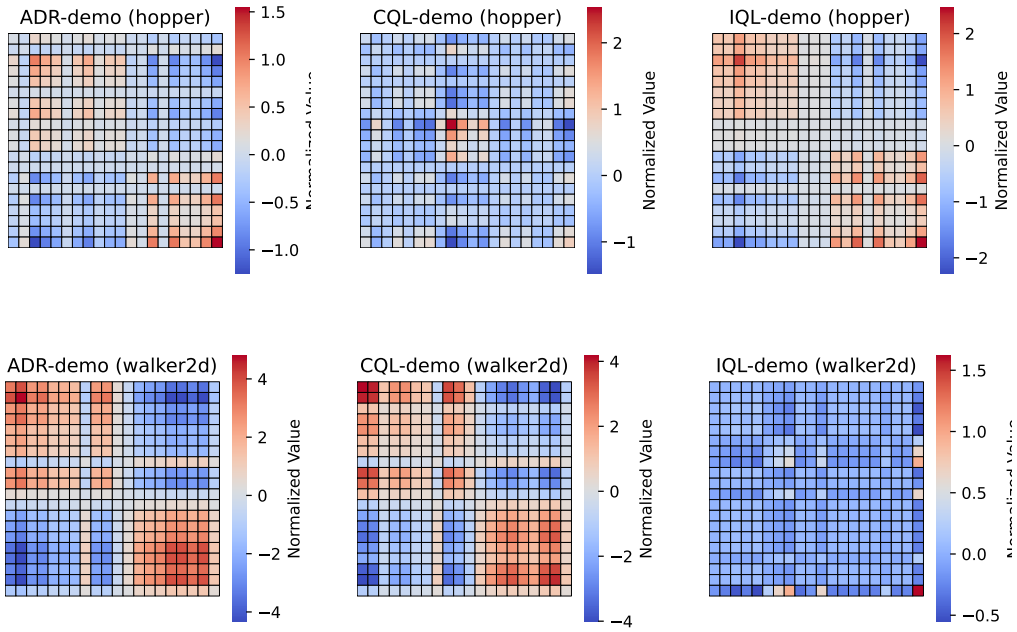

Figure 9: Heatmap of policy distributions. Higher values along the diagonal indicate a better fit of the policy to the expert policy, while lower values outside the diagonal indicate lower OOD risk for the policy.

We collect action prediction by inputting the sampled states into three models obtained by train (ADR, IQL and CQL) respectively. And after obtaining the actions, we reduce them to one dimension using PCA. Subsequently, we stack the collected actions together with the actions from the same time steps in the sampled expert dataset, calculate the covariance matrix, and then plot a heatmap to obtain Figure 9. Specifically, since the format of the dataset is `[model prediction, demo]`, only the top-left and bottom-right quarters of the heatmap have higher correlation values, which are higher than the correlations in the remaining positions of the heatmap.

For convenience, we name each heatmap plot as 'Algorithm-Demo'. From the plots, we can observe that ADR learns relatively good patterns on both the hopper and walker2d tasks, while CQL and IQL can only learn specific patterns respectively.